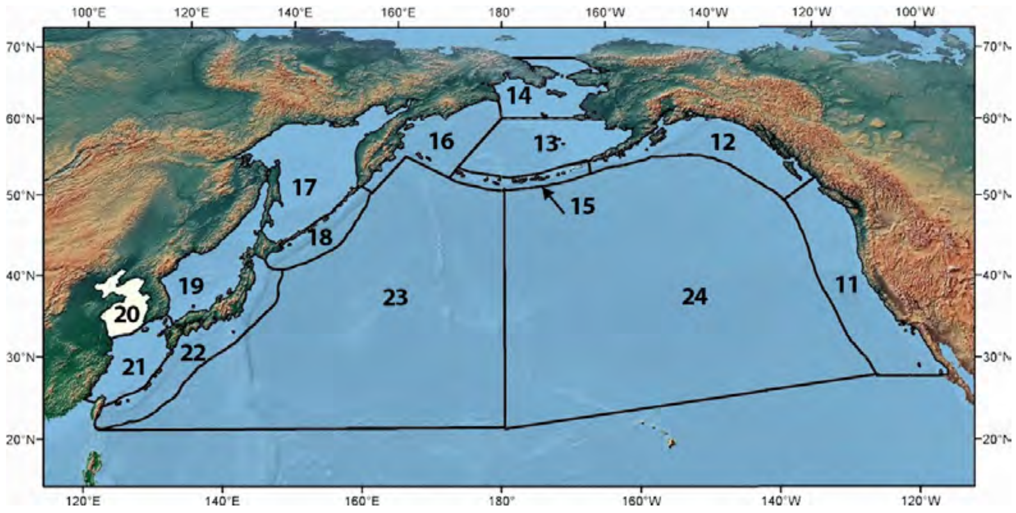

PICES

Regional Report for PICES Region:

20

PICES SPECIAL PUBLICATION 7

Marine Ecosystems of the North Pacific Ocean 2009–2016

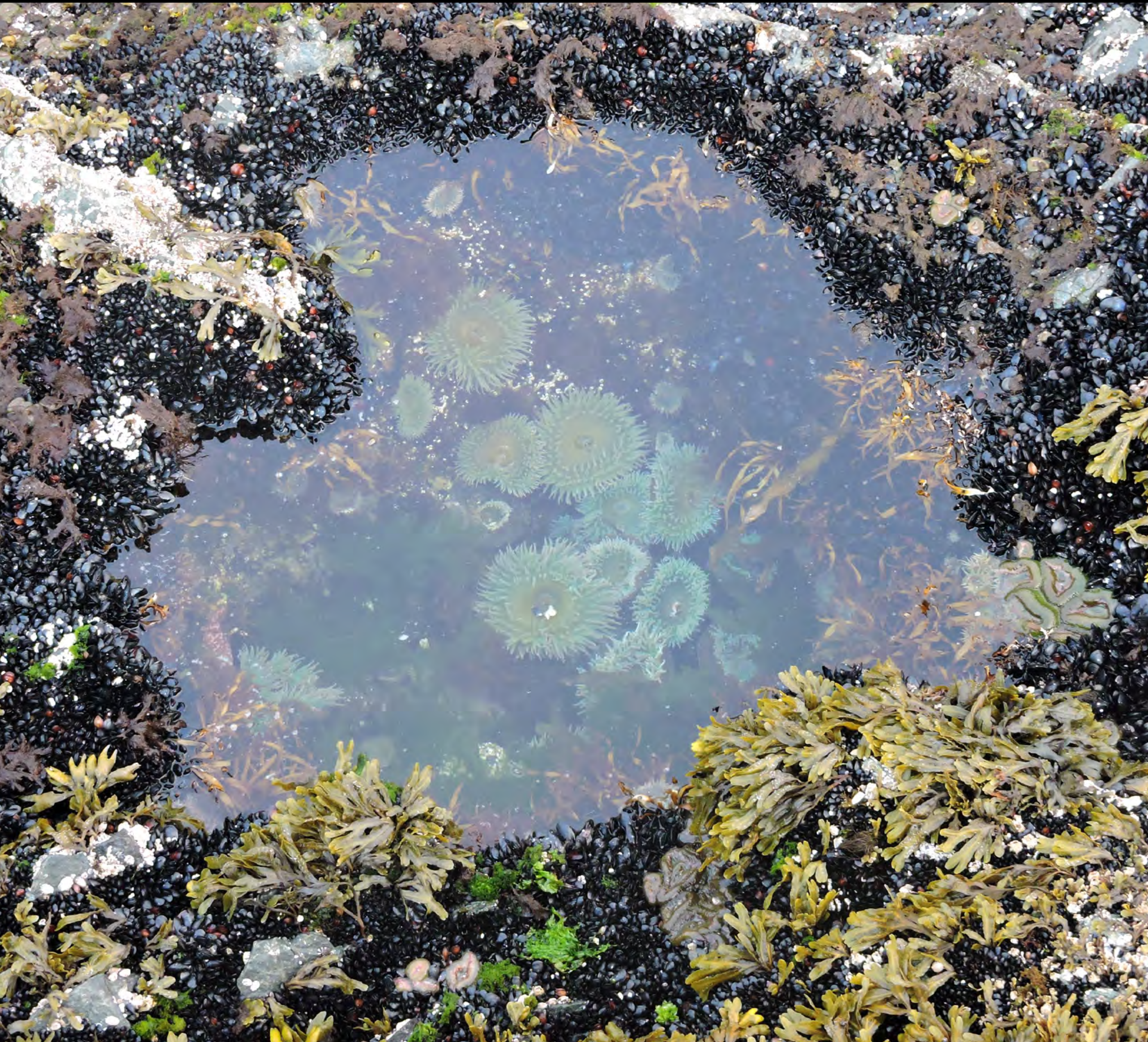

PICES North Pacific Ecosystem Status Report, Region 20 (Yellow Sea)

Sinjae Yoo[1]

Contributors:

Ahn, S.[1], Choi, M.[2], Guan, C.[3], Han, C. H.[2], Huo, C.[3], Hwang, D.-W.[2], Jung, S.[4], Kang, Y.S.[5], Khim, J.[6], Kim, H.W.[7], Kim, M.[8], Kong, C.E.[1], Lee, Y.-W.[9], Li, R.[3], Lim, W.-A.[2], Moon, H.-B.[10], Mu, J.[11], Na, G.[3], Sohn, H.[7], Sun, S.[12], Sun, X.[12], Wei, Q., Yao, Y.[3], Yeh, S.-W.[10]

[1]Korea Institute of Ocean Science and Technology (KIOST), Jeju, Korea
[2]National Institute of Fisheries Science, Busan, Korea
[3]National Marine Environmental Monitoring Center, Dalian, China
[4]Jeju National University, Jeju, Korea
[5]Korea Fisheries Resource Agency, Busan, Korea
[6]Seoul National University, Seoul, Korea
[7]National Institute of Fisheries Science, Ulsan, Korea
[8]Seabirds Lab. of Korea, Wonju, Korea
[9]Korea Marine Environment Management Corporation, Busan, Korea
[10] Hanyang University, Ansan, Republic of Korea
[11]Minjiang University, Fuzhou, China
[12]Institute of Oceanology, Chinese Academy of Science, Qingdao, China
[13]First Institute of Oceanography, State Oceanic Administration, Qingdao, China

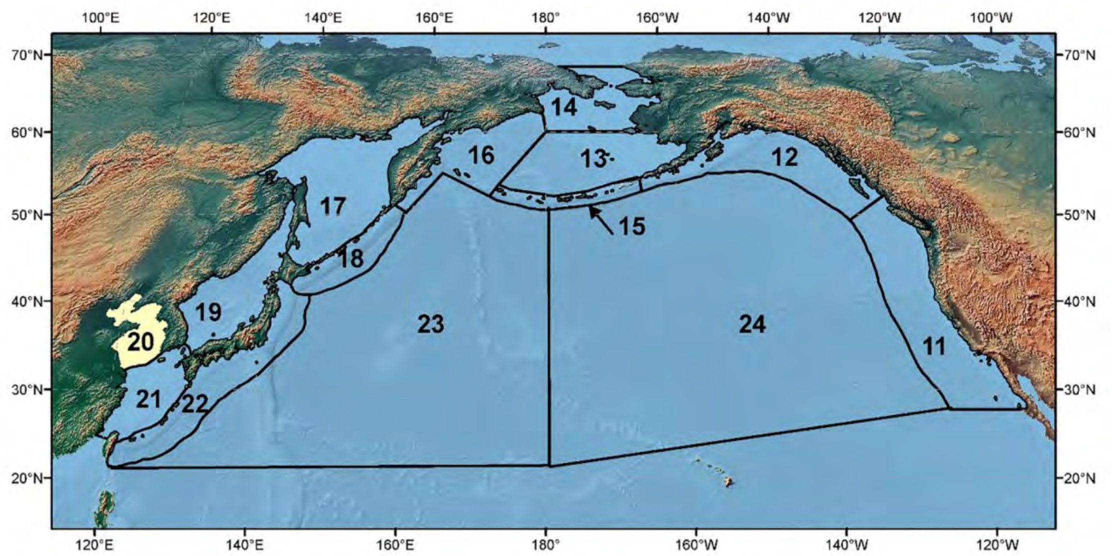

Figure R20-1. The PICES biogeographical regions and naming convention for the North Pacific Ocean with the area discussed in this report highlighted.

Highlights

- The warming in the Northwestern Pacific which began in late 1980s stopped after early 2000s, after which no particular climate pattern has been observed.
- Eutrophication in the Yellow Sea as a whole has been progressing as witnessed by the nutrient concentrations, chlorophyll-a, primary productivity, DO, and macroalgal blooms.
- The incidence of the outbreaks of HABs and large jellyfish has decreased for the past 10 years.
- No significant changes have been observed in the macrobenthos communities, shorebird populations, and spotted seals (*Phoca larga*).
- Most contaminant (POPs, PAHs, Hg) levels are safe and stable except for a few hotspots in the Chinese and Korean coasts.

1 Introduction

The Yellow Sea is a shallow marginal sea in the western North Pacific with a surface area of 380,000 km² and an average depth of 44 m (Figure R20-2). It is broadly connected with the East China Sea to the south and contains a semi-enclosed gulf in the north, the Bohai Sea. The region is one of the more densely populated in the world with human populations organized as the Peoples Republic of China, Democratic People's Republic of Korea, and the Republic of Korea, two of which are PICES member nations. The surface circulation in the region has three main currents: Kuroshio, Tsushima and the Yellow Sea Warm Current (YSWC). The Kuroshio enters the East China Sea through the strait between Taiwan and Yonakunijima Island (the eastern most of the Ryukyu Islands) and flows north-eastward along the shelf slope before branching into Tsushima Strait. The YSWC flows into the Yellow Sea after separating from the Tsushima Current west of Jeju Island. There are varying opinions regarding the origins of the Tsushima Current and YSWC (Beardsley et al. 1985; Lie and Cho 2002; Ichikawa and Beardsley 2002).

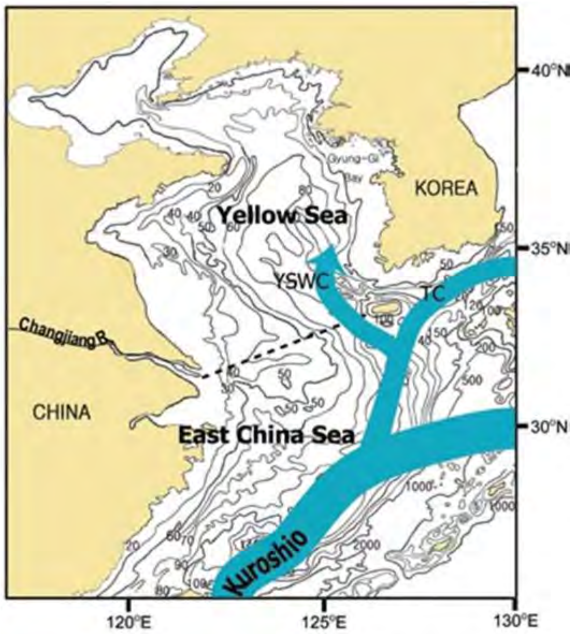

Figure R20-2. Geography, bathymetry and major currents of the Yellow Sea and East China Sea. YSWC=Yellow Sea Warm Current. TC=Tsushima Current.

The Yellow Sea is characterized by a diversity of marine habitats due to its jagged coastline and the many islands scattered around the shallow sea. Intertidal flats are the most significant type of coastal habitat. Several different types can be found, such as mudflats, salt marshes, sand flats with gravel beaches, sand dunes or eelgrass beds, and mixed flats. These habitats support important food resources and an ecological niche for a diversity of organisms. They are an important part of the Australia-East Asia flyway providing the feeding, wintering and summering grounds for migratory birds. The shallow coastal areas, encompassing more than 1,000 islands, also show high productivity and provide good nursery and fishing grounds.

The Yellow Sea is productive, supplying a large portion of the protein to human diets in the surrounding nations. The primary productivity of this sea had been estimated to be in the range of 150-200 $gC \cdot m^{-2} \cdot yr^{-1}$ (Yoo et al., 2019) and is increasing possibly due to eutrophication. Approximately 1,600 species were reported from marine and coastal habitats in the Korean part of the Yellow Sea, including 400 phytoplankton, 300 marine macroalgae, 50 halophytes, 500 marine invertebrates, and some 389 vertebrate species (Kim and Khang 2000). Among them, 166 zooplankton and 276 fish have been reported as resident species in the Yellow Sea. Approximately 100 commercial species have been identified in the region, comprising demersal fish (66%), pelagic fish (18%), cephalopods (7%), and crustaceans (7%).

However, various human activities threaten the region. The Yellow Sea is among those facing all conceivable stresses, whether natural or anthropogenic. The coastal regions of the Yellow Sea are densely populated, with approximately 600 million humans living in the region, and most of their by-products drain into the Yellow Sea. There is clear evidence of eutrophication. Artificial jetties and dams have interfered with local circulation and freshwater inputs into the sea. Overfishing has changed the trophic structure which cascades down the food web. Warming is evident. All in all, significant changes in the ecosystem are anticipated and there have been many signs. This chapter provides a review of marine ecosystem variability, with special attention to the period from 2009-2015, hereafter, the focus period.

2 Atmosphere and hydrology

2.1 Wind and Pressure

The Yellow Sea region is located where the Siberian High and the Subtropical Pacific Low collide to produce cold-dry winters and warm-wet summers. North and northwest winds in the autumn and winter are strong, with maximum speeds reaching 10 $m \cdot s^{-1}$. In the spring and summer, monsoon winds reverse the direction and become weaker. Typhoons develop in the western Subtropical Pacific bringing heavy rains in the summer and autumn. On average, about nine typhoons pass the region every year.

The long-term change in sea level pressure showed an interesting pattern. The 2nd EOF of sea level pressure (SLP) over the North Pacific, which describes the North Pacific Oscillation (NPO) (Rogers 1981), shows a shift from low pressure to higher pressure in the YECS in the middle of 1980s (Figure R20-3a), which is consistent with a warming in the YECS. In addition, the 9-year running mean of principal component time series in the 2nd EOF of SLP indicates that the phase of NPO is changing from positive to negative in the recent past. This might be associated with a slowdown of warming in the YECS (Figure R20-3b). This suggests that the circulation anomalies and thermal advection associated with the NPO-like variability in SLP play a role to increase the mean SST in the YECS since the mid-1980s.

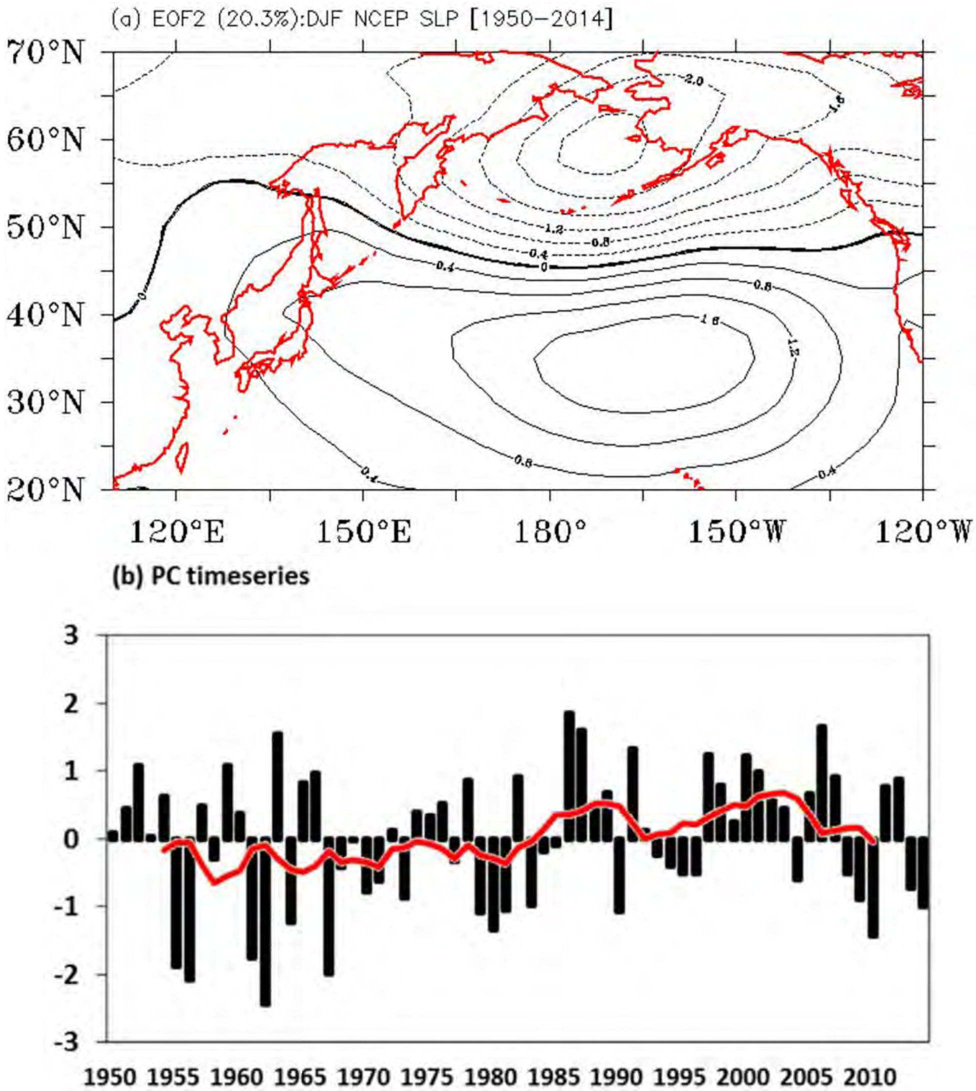

Figure R20-3. (a) The from 1950 to 2014 in the North Pacific.2nd EOF and (b) time series of PC scores of SLP in Dec-Jan-Feb

2.2 Precipitation and hydrology

The precipitation pattern over the Yellow Sea shows a typical Northeast Asian monsoon pattern according to the NOAA/Climate Prediction Center Merged Analysis of Precipitation (CMAP, http://www.cpc.ncep.noaa.gov/products/global_precip/html/wpage.cmap.html). The region has dry winters with the annual precipitation minimum (1.1 mm·d^{-1}) in December and wet summers with the maximum precipitation (5.5 mm·d^{-1}) occurring in July for the period 1979-2017 (Figure R20-4). During the same period, there was an increase from 2003 to 2013 (Figure R20-5).

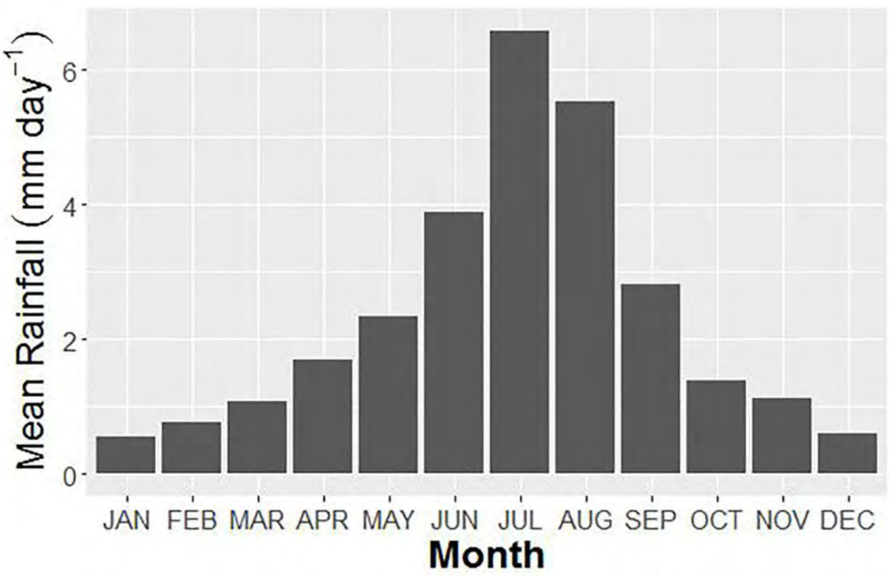

Figure R20-4. Monthly precipitation over the Yellow Sea area averaged for 1979-2017. The pattern shows a typical northeastern Asian monsoon pattern of dry winters and wet summers. CMAP data are used.

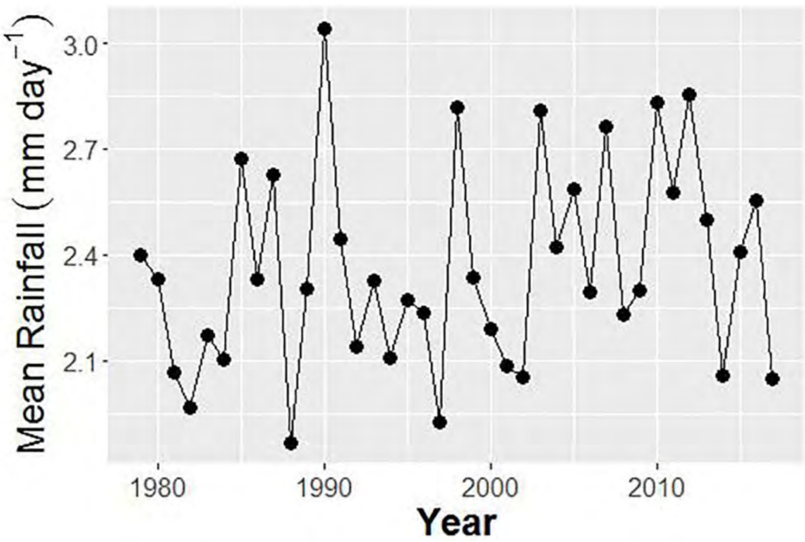

Figure R20-5. Annual average precipitation over the Yellow Sea area. CMAP data are used.

Fourteen rivers drain into the Yellow and East China seas, with a total discharge of $>10^{12}$ $m^3 \cdot y^{-1}$ (Hong et al. 2003). Of these, the Changjiang River has the largest discharge ($895 \times 10^9 \cdot m^3 \cdot y^{-1}$). During the summer monsoon, salinity drops by as much as 6 psu. Such abrupt events have devastating effects on aquaculture and on some parts of the adjacent ecosystem.

3 Physical and Chemical Ocean

3.1 Hydrography

The most striking feature in the region (32°N-40°N, 118°E-127°E) is how its surface waters have warmed during boreal winter since the mid-1980s (Figure R20-6). Figure R20-6 shows the time series of averaged SST over the Yellow Sea and East China Sea (YECS) (25°N-40°N, 118°E-127°E) during the boreal winter for 1950-2014. Note that the red line in Figure R20-6 indicates a 9-year running mean time series and the boreal winter is defined as the three months from December to February in the following year. In details, the 9-year running mean time series indicates that the mean SST in the YECS has gradually increased since the mid and late 1980s, however, such a warming trend is slowing down recently. This indicates that there exists a decadal variability of SST in the YECS, which is closely associated with Pacific Decadal Oscillation, the Kuroshio transport and the intensity of Siberian High pressure (Kim et al. 2018). In spite of this, the long-term trend of SST in the YECS shows two distinctive periods during 1950-2014. The first was a cold period up to the mid-1980s, when it shifted to a warming period (Figure R20-6). This warming in the YECS seems to be associated with large scale atmospheric variability over the North Pacific basin (Yeh and Kim 2010). An EOF analysis showed that the warming trend is most conspicuous on the shelf area of the East China Sea and the central Yellow Sea (Figure R20-7a). The dominant sign of the first EOF principal component time series changes from negative to positive before and after the mid-1980s, respectively (Figure R20-7b).

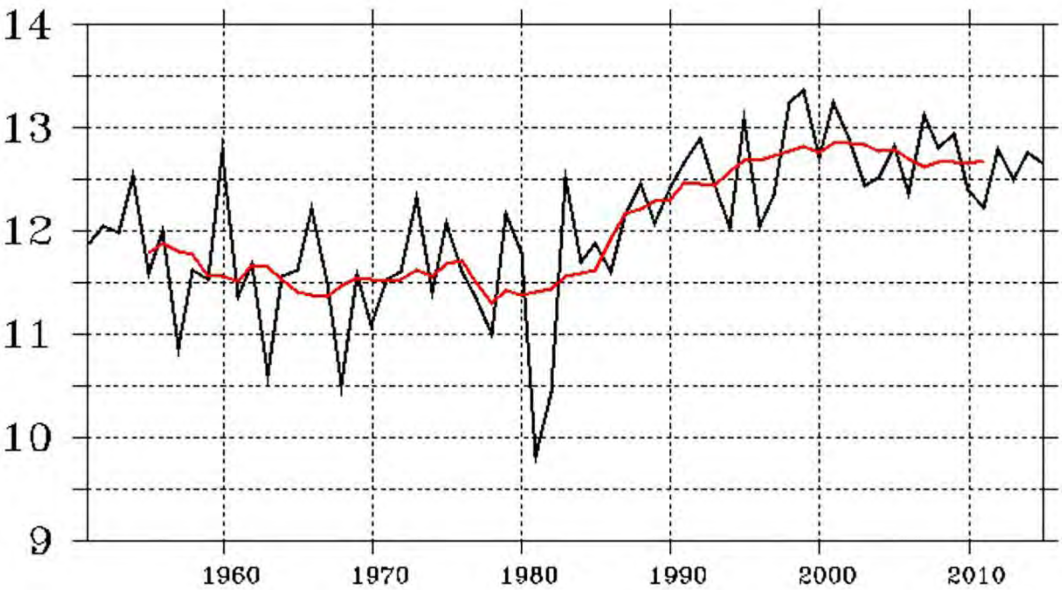

Figure R20-6. The trend of SST (Hadley Centre) in Dec-Jan-Feb from 1950 to 2014 in the Yellow Sea and East China Sea region (25°N-40°N, 118°E-127°E). A warming trend was evident from the mid-1980s until the early 2000s. The thick line indicates a nine-year moving average.

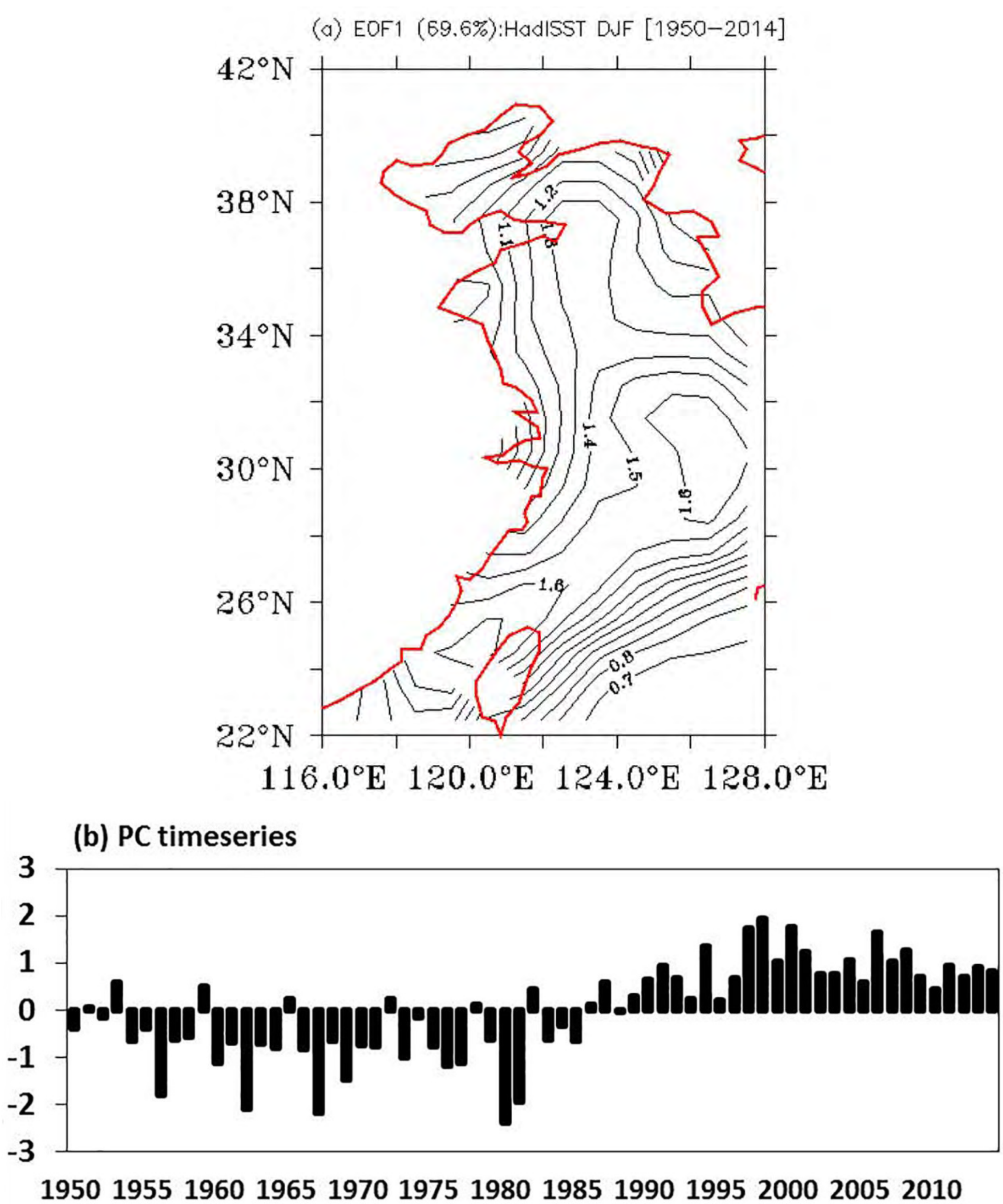

Figure R20-7. (a) The 1st EOF and (b) time series of PC scores of SST (Hadley Centre) in Dec-Jan-Feb from 1950 to 2014 in the Yellow Sea and East China Sea region (25N-40N, 118E-127E).

Figure R20-8 shows a time series of the mean near-surface sea temperature extracted from 25 stations in a rectangular area (35°N-37°N, 123.5°E-125.5°E) in the central southern Yellow Sea. Here, the warming described above can be seen starting from 1989. The temperature difference between 0 m and 45-50 m depth in August, as a proxy of stratification strength, shows stratification has been strengthened after 1995 (Figure R20-9). The near-surface salinity in August shows that the surface layer has freshened after 1998. These data indicate that the system underwent a shift in temperature and salinity in the late 1980s through middle 1990s. However, after this shift there has been no particular trend.

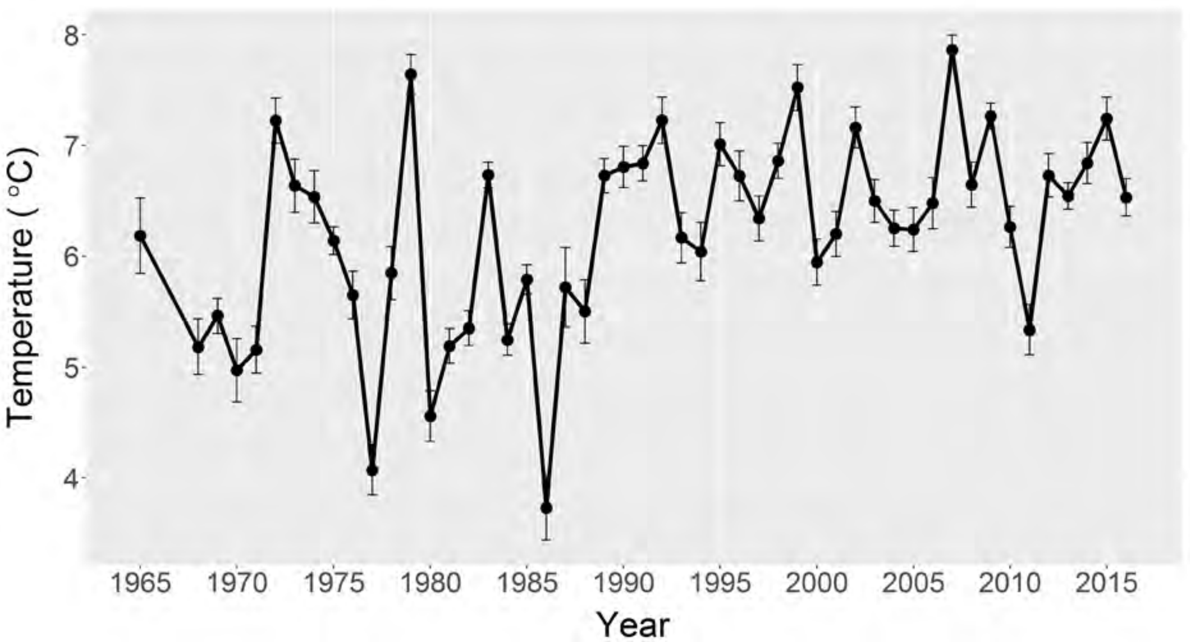

Figure R20-8. The trend of near-surface sea temperature in February in the central Yellow Sea. The vertical bars represent the standard deviation.

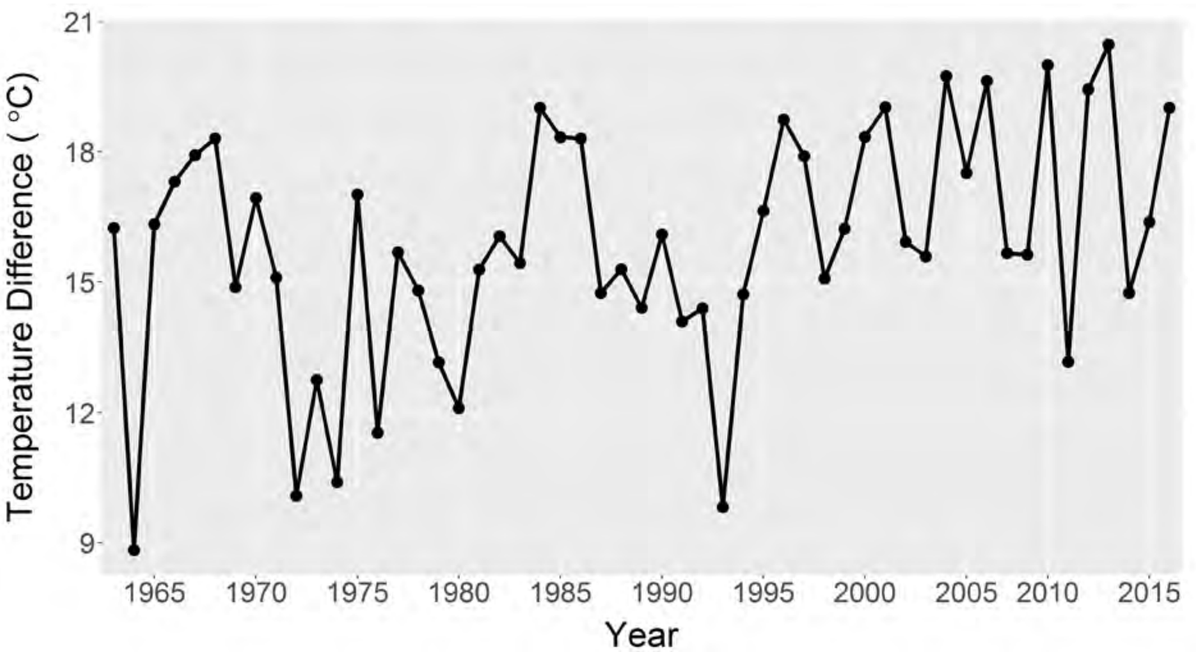

Figure R20-9. The sea water temperature difference between 0m and 45-50m in August in the central Yellow Sea.

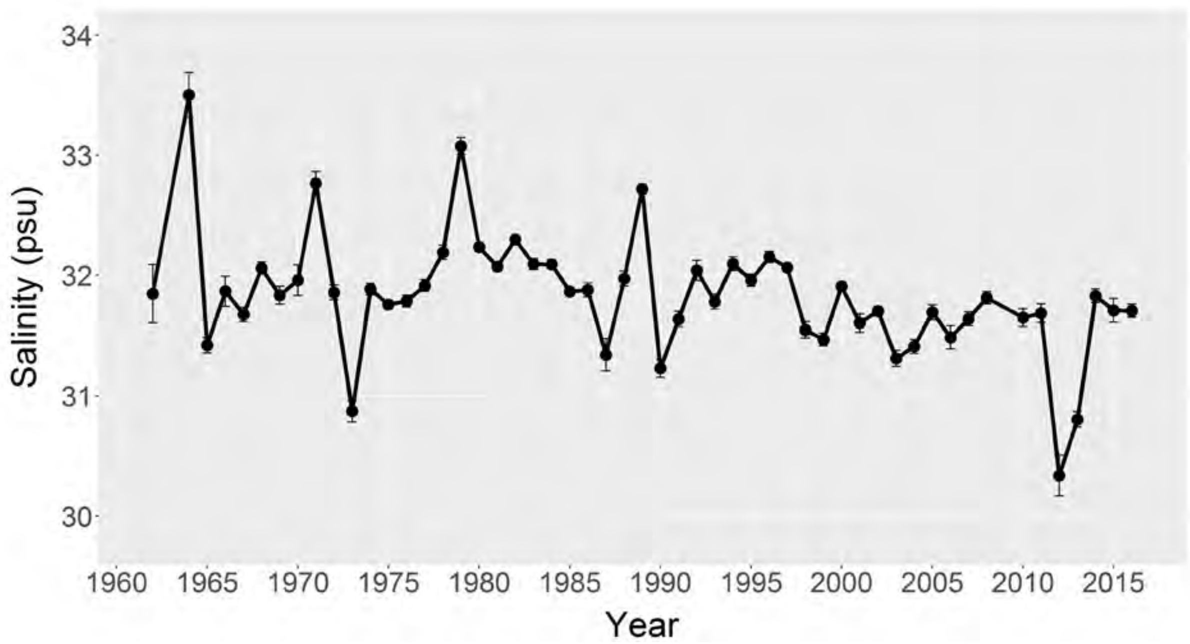

Figure R20-10. The trend of near-surface salinity in August in the central Yellow Sea. . The vertical bars represent the standard deviation.

4 Chemical Ocean

4.1 Oxygen, carbonate system, and pH

A survey in August 2008 found that the dissolved oxygen (DO) concentrations ranged from <2.0 mg·l^{-1} to >5.0 mg·l^{-1} in the bottom layer of the basin (YSLME 2010). Except for the station in the vicinity of the Changjiang river mouth, DO was >2.0 mg·l^{-1} in most regions. One of the largest coastal low-oxygen areas in the world occurs in the vicinity of the Changjiang River mouth (Chen et al. 2007). In August 2003, the area of DO concentrations <2-3 mg·l^{-1} covered >12,000 km^2. Hypoxia occurs near the Changjiang River mouth due to strong stratification and high primary production (Rabouille et al. 2008). The basin-wide survey in October 2003 also showed that pH values ranged from 7.63 to 8.17 with an average of 8.02 (KCJRG 2004). The pH was slightly higher on the surface than it was at a depth of 50 m.

In the northern Yellow Sea, the surveys during 2011-2012 (Zhai et al. 2014) showed that, the fugacity of CO_2 (fCO_2) of bottom water gradually increased from 438±44 μatm to 630±84 μatm, and pH_T decreased from 8.02±0.04 to 7.88±0.06 from July to October due to local aerobic remineralization of primary-production-induced biogenic particles. The subsurface community respiration rates in summer and autumn were estimated to be from 0.80 to 1.08 μmol O_2 kg^{-1} d^{-1} within a relatively high salinity range of 31.63 to 32.25 psu. From November to May in the next year, however, subsurface fCO_2 gradually decreased and pH increased due to cooling and water column ventilation. In the corresponding bottom water, the carbonate saturation state of aragonite (Ω_{arag}) was 1.85±0.21 (May), 1.79±0.24 (June), 1.75±0.27 (July), 1.76±0.29 (August), 1.45±0.31 (October), 1.52±0.25 (November), and 1.41±0.12 (January). Extremely low Ω_{arag} values (from 1.13 to 1.40) were observed mainly in subsurface waters within the high salinity range of 31.63 to 32.25, which covered a major fraction of the survey area in October and November. In summer, surface water Ω_{arag} ranged from 2.1–4.2, enhanced by biological production. However, subsurface water Ω_{arag} was lower than 2.0 and had its lowest value of 1.1 at a central northern Yellow Sea station (38° 40′ N, 122° 10′ E). From the surveys above, the surface dissolved oxygen was saturated from March to August and nearly in equilibrium with the atmosphere from September to October. During November and January, dissolved oxygen declined to an undersaturated level. In contrast, saturation state of aragonite increased from spring and reached its highest values in summer. In autumn, it declined slightly to a level just higher than spring and it reached the lowest level in winter.

Li et al. (2015) analyzed the long-term trend in nutrients and DO in the southern Yellow Sea (SYS) from the 1980s to 2012 using field and historical data. The annual mean DO concentration was relatively constant until 2000 and became lower since 2008 (Figure R20-11F). In the southern Yellow Sea, the DO concentration has not reached a hypoxia level (<6 mg L^{-1}) as of 2012.

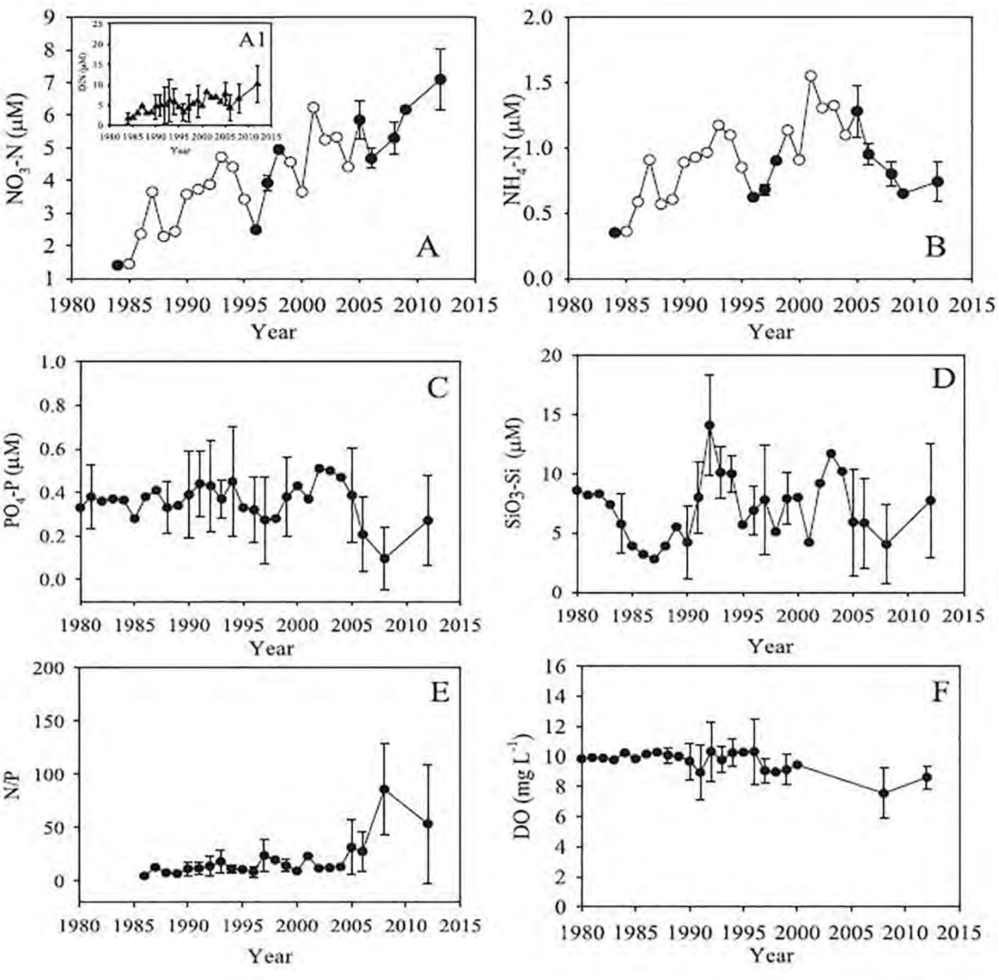

Figure R20-11. Annual variation in NO_3-N, DIN (the inset in figure A), NH_4-N (DIN), PO_4-P, SiO_3-Si, the N/P ratio, and DO concentrations in the SYS from the 1980s to 2012 (Note: The data represent average values ± the standard deviation during different years in the study area; in figures A and B, the filled and open circles stand for the field and computational data, respectively) (Li et al. 2015).

4.2 Nutrients

Figure R20-12 shows the long-term variation (1976–2006) of nutrient concentrations and nutrient ratios along the 36˚N transect in winter (Wei et al., 2015). Overall, the patterns of nutrient concentrations and nutrient ratios were similar in winter and summer (data not shown). The concentrations of dissolved organic nitrogen (DIN) in the southern Yellow Sea had been continuously increasing in recent decades. However, the concentrations of PO_4-P and SiO_3-Si (especially the SiO_3-Si) initially decreased from the 1970s to the mid-1990s and then increased. The N/P ratio increased continuously and became greater than 16 at the beginning of the 21st century, but the Si/N ratio decreased rapidly from the mid-1980s and then maintained a low value at the beginning of the 21st century. The Si/P ratio decreased from the 1970s to the mid-1990s and then started to increase gradually. Consequently, there was a progressive trend from an early N limitation to the current potential P and Si limitation in the southern Yellow Sea.

As discussed by Wei et al. (2015), the variations of the nutrient concentrations in the southern Yellow Sea were related to the variations of the riverine flux and atmospheric deposition, and especially the long-term variations of SiO_3-Si and PO_4-P concentrations were both generally consistent with the variation of precipitation (Wei et al. 2015). In addition, the nutrient transport by the inflow from the outer shelf of the East China Sea, in combination with the anthropogenic eutrophication in the coastal zones, may also influence the nutrient levels in the southern Yellow Sea under the global change.

The study conducted by Fu et al. (2012) also showed that the water column concentrations of DIN, PO_4-P and SiO_3-Si along the 36˚N transect in the area west of 124.5˚E increased in 2007 and 2008 compared to those in the 1990s. These studies provided additional examples of the increase in the concentrations of PO_4-P and SiO_3-Si and the continuous increase in the concentration of DIN in the Yellow Sea since the late 1990s. Li et al. (2015) have shown that in the southern Yellow Sea, nitrate has increased continuously as of 2012 and phosphates decreased after 2005 (Figure R20-11A and Figure R20-11C). As a result, N/P ratio has drastically increased after 2005 in the southern Yellow Sea (Figure R20-11E).

However, a recent study suggests that this long-term trend of increasing trend may have ceased after 2011. The YSLME (Yellow Sea Large Marine Ecosystem) Project analysed the nutrient data collected by the Chinese National Marine Ecology Environmental Monitoring Network (Working Group on Governance of the PR China, 2019). The data set covers the northern as well as southern Yellow Sea of the Chinese side of the Yellow Sea. According to their preliminary results, the annual surface DIN concentration has decreased since 2011, while the bottom concentration did not show any trend (Figure R20-13). The annual surface phosphates concentration showed peaks in 2006 and 2011 but remained stable after 2012 (Figure R20-14). Similarly, the annual bottom phosphates concentration showed a peak in 2006 but remained stable afterward. Therefore, the nitrogen enrichment consistently reported by previous studies may have lessened. Whether this is a sign of improvement in one of the serious environmental issues in the Yellow Sea remains to be further investigated.

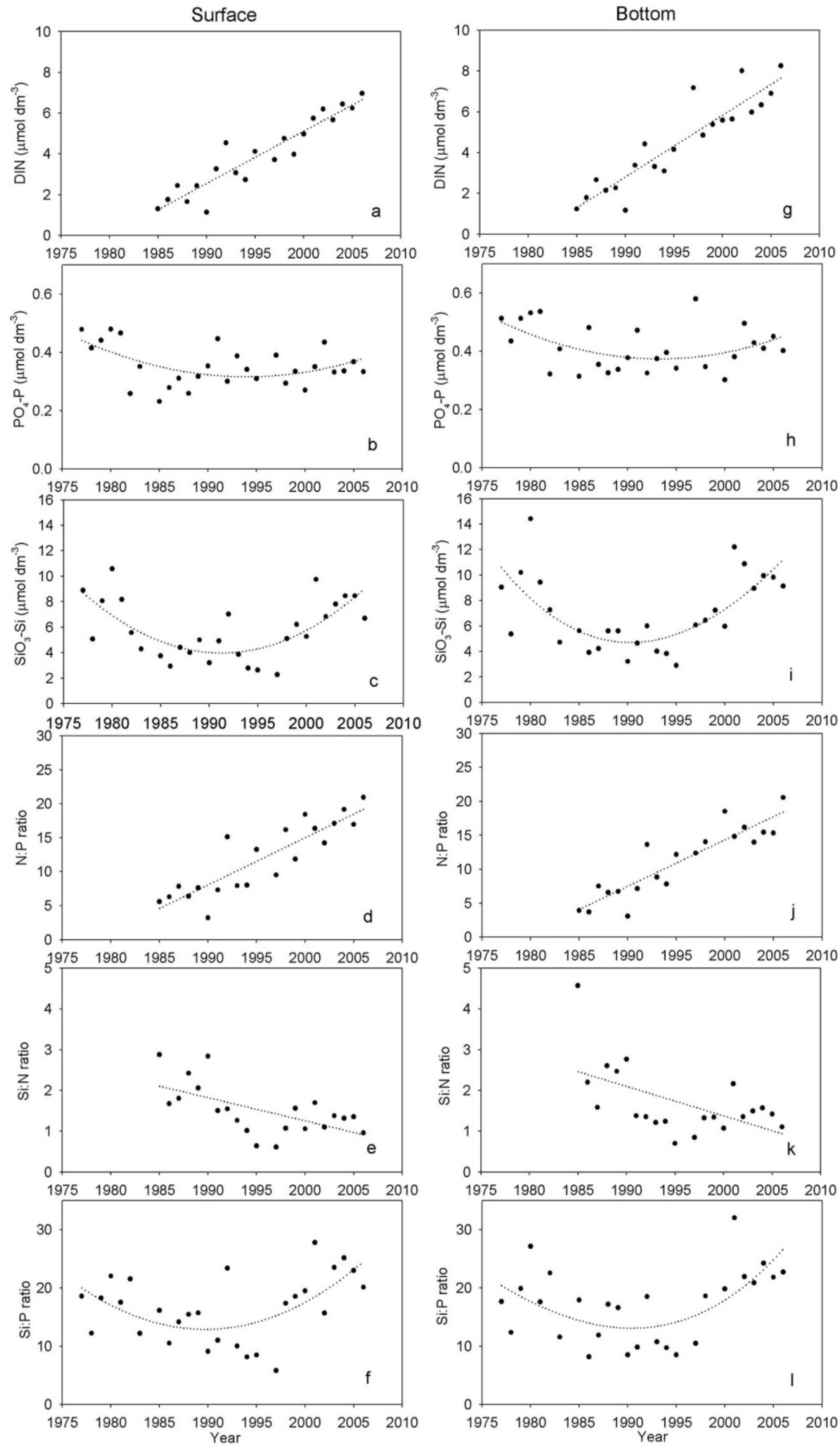

Figure R20-12. Temporal variations in nutrient concentrations and nutrient ratios in the southern Yellow Sea in winter (Wei et al. 2015).

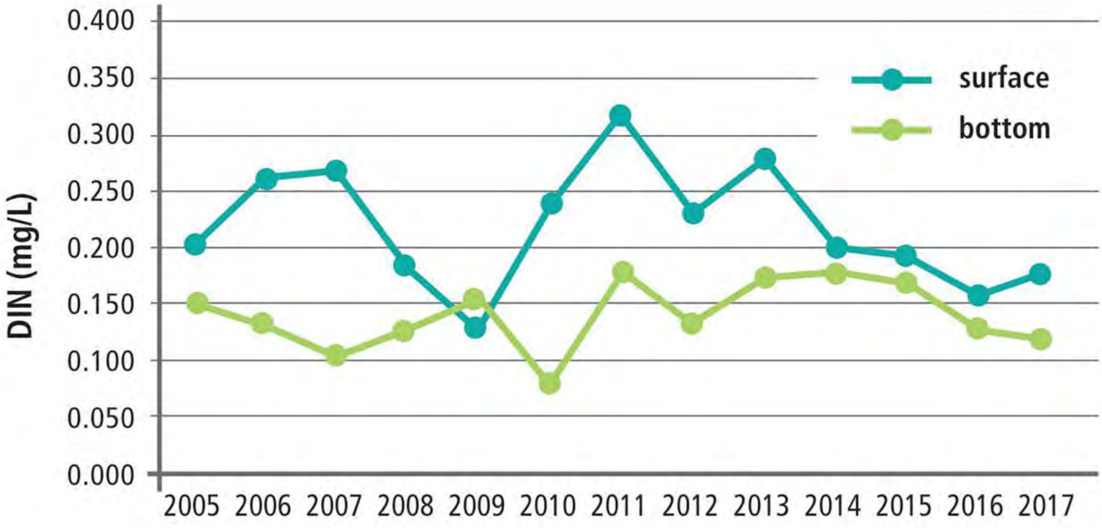

Figure R20-13. Annual changes of phosphate concentration in the Yellow Sea, surface and bottom (Working Group on Governance of the PR China, 2019).

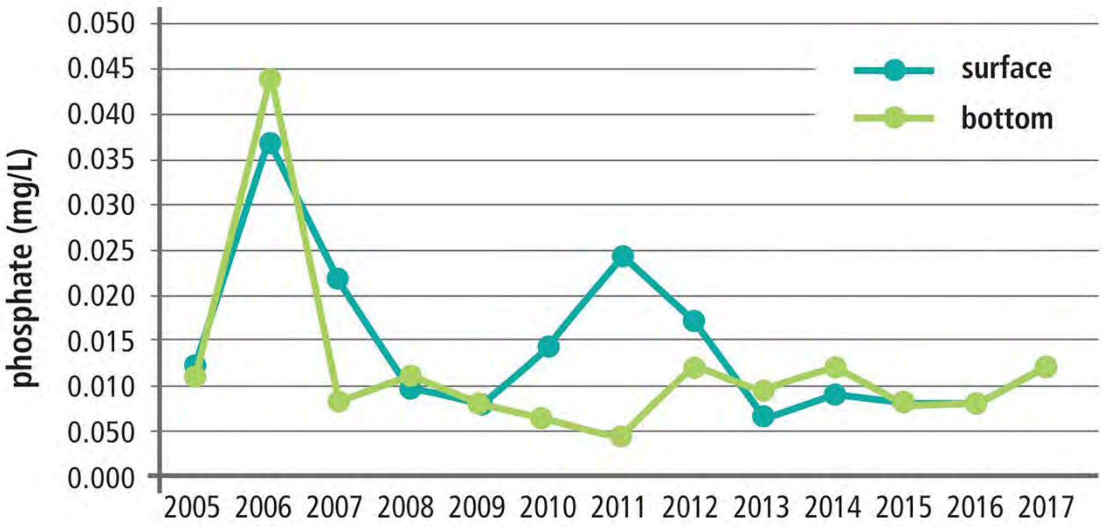

Figure R20-14. Annual changes of silicate concentration in Yellow Sea, surface and bottom (Working Group on Governance of the PR China, 2019).

5 Phytoplankton

5.1 Light

Photosynthetically Active Radiation (PAR) at the sea surface over the Yellow Sea region was estimated from SeaWiFS/MODIS data (as described in Yoo et al. 2019) for the period 1998-2014. The minimum annual average PAR was 31.1 $E{\cdot}m^{-2}{\cdot}d^{-1}$ in 2010 and the maximum was 34.1 $E{\cdot}m^{-2}{\cdot}d^{-1}$ in 2000 (Figure R20-15). During the period, PAR decreased after 2003.

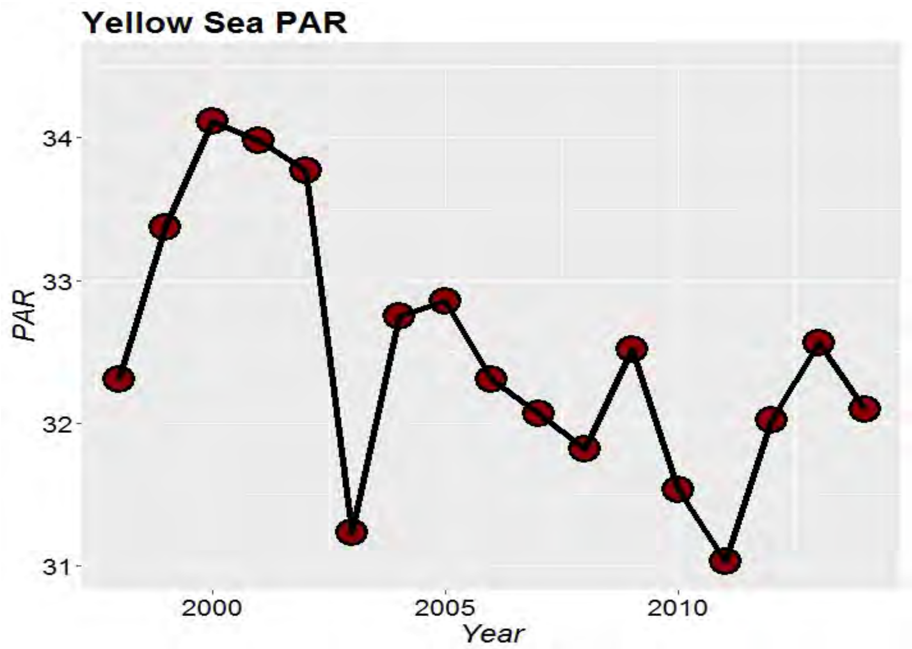

Figure R20-15. Annual averages of PAR in the Yellow Sea from 1998 to 2014.|

5.2 Phytoplankton

5.2.1 Biomass and productivity

Seasonal phytoplankton blooms are known to occur in the Yellow Sea but there are few time series to show the interannual variation in the timing and intensity of the blooms. Compiled *in situ* records show that there are great variations in the phytoplankton biomass and primary productivity in the Yellow Sea depending on the area and time. For example, the primary productivity ranged from 1.8 to 3175 $mgC \cdot m^{-2} \cdot d^{-1}$ (Yoo and Shin 1995; Cho et al. 1994; Kang et al. 1992; Choi et al. 1988; Park 2000). In open waters of the Yellow Sea where the water column is seasonally stratified at shallow depths, seasonal blooms develop in spring and autumn. A bi-monthly survey of the eastern half of the Yellow Sea in 1986 showed that mean chlorophyll-a was 1.5 $mg \cdot m^{-3}$ from 12 stations in April (0.4-3.3 $mg \cdot m^{-3}$) while in October, the mean was 0.97 $mg \cdot m^{-3}$ (range: 0.7-1.2 $mg \cdot m^{-3}$) (Choi et al. 1988). The mean values were 0.70, 0.66, and 0.4 $mg \cdot m^{-3}$, in June, August and December, respectively, showing a clear bimodal seasonal pattern. Seasonal cycles were also observed in some of the shallow tidally-mixed areas. There, timing of blooms varied depending on local conditions. In Gyung-Gi Bay (see Figure R20-2 for location), the spring bloom occurred in March and the autumn bloom early in September. Freshwater discharge probably played an important role in this area (Song 1999).

A bi-monthly survey in the eastern half of the Yellow Sea in 1987 found 394 species of phytoplankton during the year (Han and Choi 1991). More than 90% of these were diatoms and dinoflagellates and the proportion of dinoflagellates increased in stratified water. Biomass and abundance of phytoplankton were typically high in coastal areas and near the Changjiang River mouth but lower in the central areas (UNDP/GEF 2007). In the summer of 2008, chlorophyll-a concentrations varied from 0.13 $mg \cdot m^{-3}$ to 6.69 $mg \cdot m^{-3}$ with an average of 1.24 $mg \cdot m^{-3}$ (microplankton; 29%, nanoplankton; 12%, picoplankton; 59%) (YSLME 2010). In the northern part of the Yellow Sea, *Chaetoceros* spp., *cryptomonads*, *Paralia* *sulcata, Karenia mikimotoi,* and *Navicula* spp. were the dominant species. The total number of species there was 110, among which 73 species were diatoms and 29 were dinoflagellates. In the southern part of the Yellow Sea, nanoflagellates, cryptomonads, and *Prorocentrum* spp. were the dominant species. The daily primary productivity during this study was in the range from 121 $mgC{\cdot}m^{-2}{\cdot}d^{-1}$ to 1,204.7 $mgC{\cdot}m^{-2}{\cdot}d^{-1}$ with an average of 592.8 $mgC{\cdot}m^{-2}{\cdot}d^{-1}$ (YSLME 2010). Because of the high spatial and temporal variability, it is difficult to compare these results with previous studies.

In the tidally mixed zone, turbidity is very high and light could be a major limiting factor for phytoplankton growth. I_k, the light intensity of the photosynthesis saturation, was as low as 10-12 $\mu E{\cdot}m^{-2}{\cdot}s^{-1}$ in a mixed coastal area in the winter (Yoo and Shin 1995). Tycho-pelagic species such as *Paralia sulcata* were dominant and diatoms were abundant. Species diversity was usually high throughout the year with a less conspicuous seasonal pattern.

Using the best available parametrizations for the core variables in the region at present, Yoo et al. (2019) reassessed the primary productivity of the Yellow Sea for 1998-2014, and suggested an average of 219 (range: 196–244) $gC{\cdot}m^{-2}{\cdot}yr^{-1}$. During the period, the chlorophyll-a and primary productivity in the Yellow Sea steadily increased after 2003 and levelled off after 2009 (Figure R20-16 and Figure R20-17). This is in parallel with the increase in inorganic nutrients (Section 4.2). He et al. (2013) also attributed the increase in the intensity of the phytoplankton blooms to the increase in the concentrations of NO_3-N and PO_4-P in the Yellow Sea.

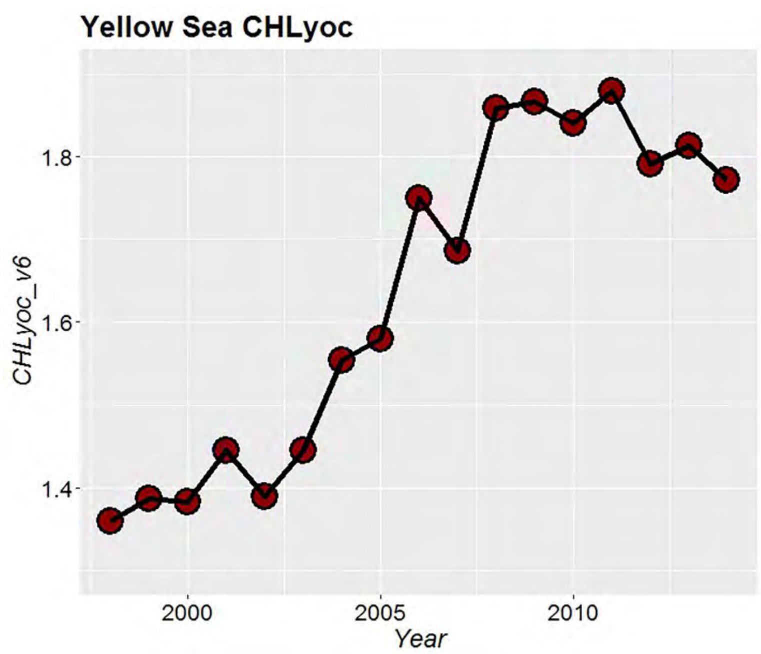

Figure R20-16. Annual averages of chlorophyll-a in the Yellow Sea from 1998 to 2014 using a region-specific chlorophyll-a algorithm (Yoo et al. 2019).

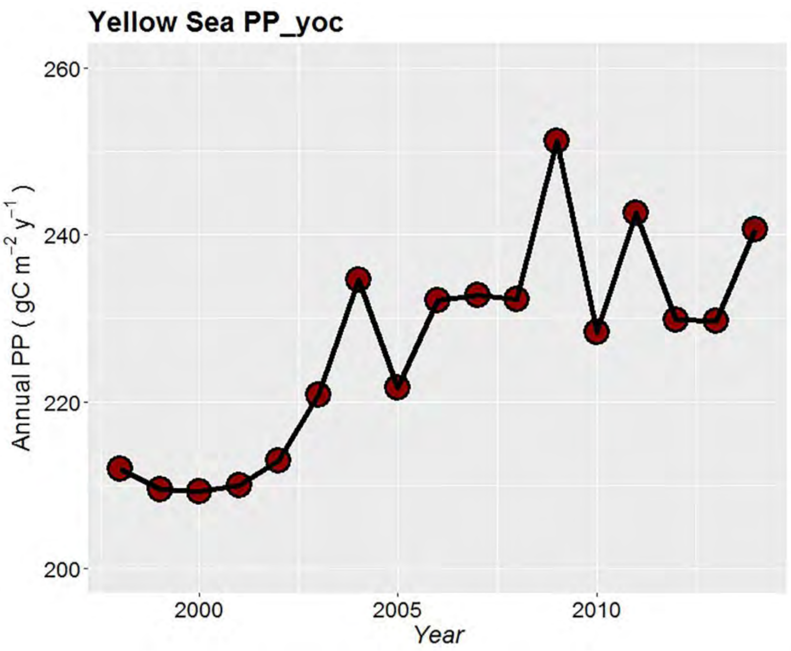

Figure R20-17. Annual averages of primary productivity in the Yellow Sea from 1998 to 2014 (Yoo et al. 2019).

5.2.2 Algal blooms

Red tides are common off the Chinese and Korean coasts and are related to the eutrophication of the Yellow Sea and East China Sea (Zhou et al. 2008; Tang et al. 2006). During the late 1990s, algal blooms (defined by cell density) in both Chinese and Korean waters increased. In the Korean waters, the number of algal blooms levelled off after 2000 but in the Chinese waters, it increased until 2009 (Figure R20-18). In both the Korean and Chinese coasts of the Yellow Sea, the number of algal blooms decreased after 2010 (Figure R20-18).

In the western coast of Korea, major red tide species were *Noctiluca scintillans*, *Mesodinium rubrum*, *Skeletonema costatum*, and *Stephanopyxis palmeriana*. Algal blooms have been decreasing since 2010 and there has been no bloom after 2013 (Figure R20-18). The proportion of major HAB species was *Chattonella* sp. (30%), *C. polykrikoides* (17%), *H. akashiwo* (13%), *S. costatum* (13%), and 6 species including *M. rubrum* were present in less than 7% during 2009-2015 (Table R20-1).

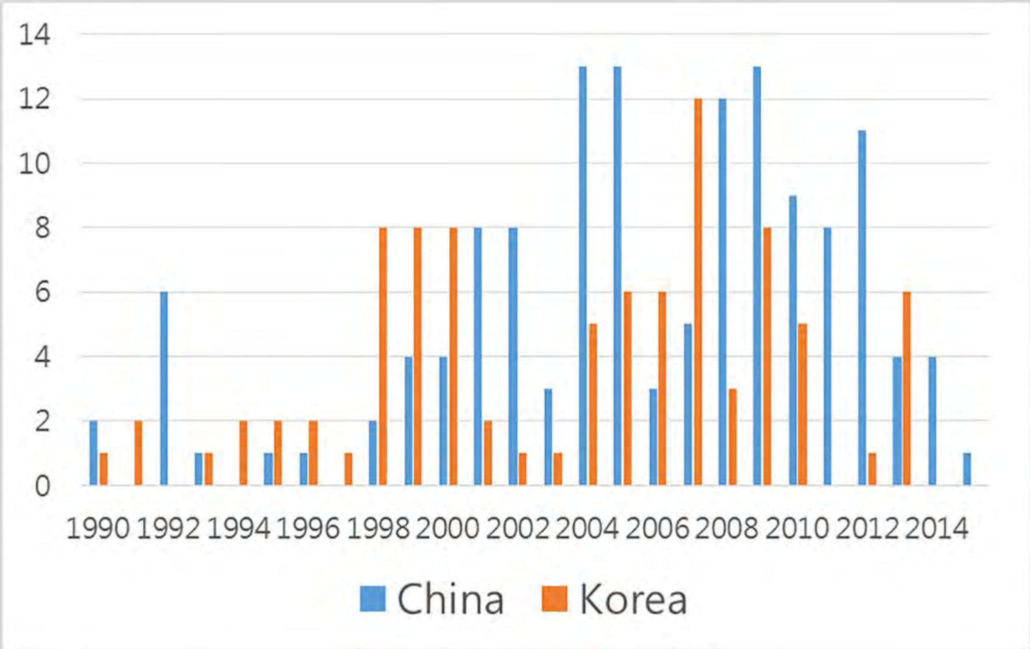

Figure R20-18. Frequency of algal blooms along the Chinese and Korean coasts in the Yellow Sea during 1999-2015.

Table R20-1. Dominant species of harmful algal blooms in the western coast of Korea during 2009-2015.

	Species of HABs	Number of events	Relative Appearance Rate (%)
Dinoflagellates	*Chattonella* sp.	9	30
	Cochlodinium polykrikoides	5	17
	Heterosigma akashiwo	4	13
	Katodinium glaucum	1	3
	Mesodinium rubrum	2	7
	Noctiluca scintillans	1	3
	Prorocentrum sp.	2	7
Diatom	*Skeletonema costatum*	4	13
	Stephanopyxis palmeriana	1	3
	Heterocapsa triquetra	1	3

On the Chinese coast of the Yellow Sea, the number and area of algal blooms did not obviously differ between 1999-2007 and 2008-2016 (Figure R20-19). From 1999 to 2007, the major species were *Noctiluca scintillans* (25%), *Gymnodinium catenatum* (14%), *Skeletonema costatum* (11%), *Akashiwo sanguinea* (11%), *Mesodinium rubrum* (11%), *Thalassiosira* spp. (8%), *Heterosigma akashiwo* (8%), *Eucampia* spp. (6%). From 2008 to 2016, the major species were *Noctiluca scintillans* (43%), *Skeletonema costatum* (18%), *Chattonella marina* (12%), *Heterosigma akashiwo* (10%), *Akashiwo sanguinea* (6%). While *Gymnodinium catenatum* and *Mesodinium rubrum* decreased, *Noctiluca scintillans*, *Skeletonema costatum* and *Chattonella marina* increased. From 1972 to 2016, May-September was the peak season of algal blooms in the Chinese coastal waters (Figure R20-20). The number of algal blooms was higher in May, August and September, and the cumulative area was the largest in May. The number and area of algal blooms in these five months were accounted for 85.3% and 95.1% of the total algal blooms in the whole year, respectively. From October to April of the following year, algal blooms rarely occurred in the Yellow Sea.

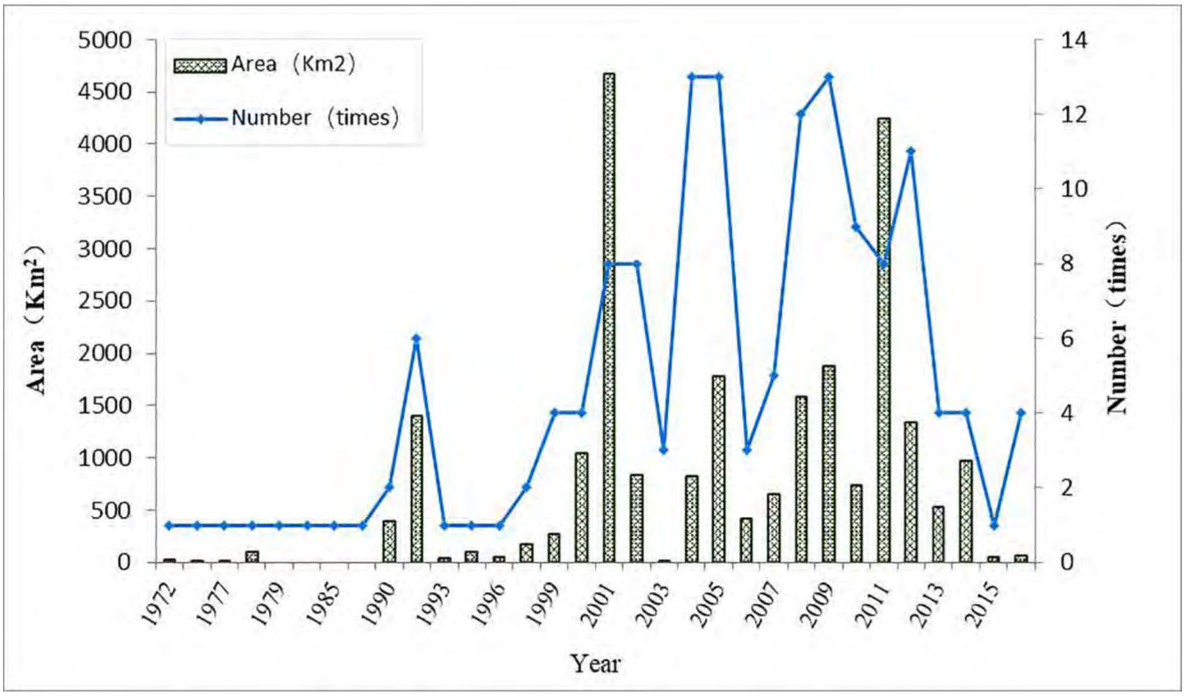

Figure R20-19. Trends of algal blooms in Yellow Sea of China from 1972-2016.

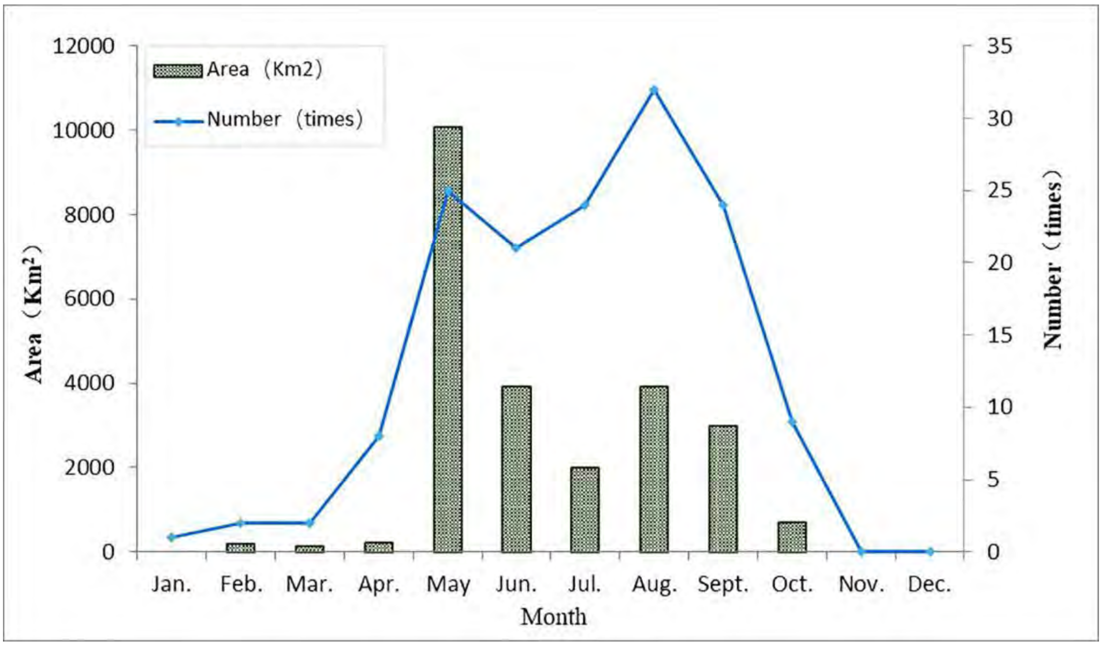

Figure R20-20. Trends of algal blooms in Yellow Sea of China in different months from 1972-2016.

5.2.3 Green tides

The increase in the frequency of occurrence, intensity and geographical range of ephemeral macro-algal blooms is a widespread symptom of chronic eutrophication in coastal areas (Schramm 1999; Jones and Pinn 2006; Zhou et al. 2015). In the last decade, the Chinese coastal waters in the Yellow Sea of has experienced the world's largest green tide (Liu et al. 2013; Wang et al. 2015; Xing et al. 2015). In 2007, a green tide was observed for the first time on a small scale in the center of the Yellow Sea (Sun et al. 2008). The green tide began to attract much attention in 2008 by invading the Olympic Sailing Course in Qingdao. Since then, the green tides showed up every year in the western coast of the Yellow Sea during the spring-summer period. The annual (May-August) mean area of green tides shows dramatic changes between 2007 and 2015 in both the algal distribution and coverage (Qi et al. 2016). In recent years, the maximum area shows an increasing trend (Figure R20-21).

According to the previous studies, these opportunistic macroalgal blooms have various direct and indirect effects on ecosystem structure and function, as they can alter physical and biological variables by forming mats with their abundant and dense canopies (Hauxwell et al. 2001; Jones and Pinn 2006; Le Luherne et al. 2016). Generally, macroalgal mats cause the underlying sediments to become more reducing, often leading to anoxia and accumulation of toxic hydrogen sulphide, consequently posing a potential threat to the structure and function of the coastal ecosystem (Cabral et al. 1999; Bolam et al. 2000; Garcia-Robledo et al. 2012).

It is still not clear what the long-term ecological impact of the annual large-scale green tides is (Wang et al. 2015), though significant social and economic losses had emerged due to the large piling up of algal biomass on beaches and coastal waters of both Shangdong and Jiangsu provinces (Ye et al. 2011). It cost nearly 100 million USD for cleaning of algae offshore of Qingdao in summer 2008 to achieve Olympic Games standards (Wang et al. 2009b). Meanwhile, it has caused direct aquaculture losses of 116 million USD along the green-tide-affected coastlines (Ye et al. 2011).

It should be noted that the blooms of macroalgae tend to last much longer than short-lived blooms of dinoflagellates or other microalgae (Valiela et al. 1997). Thus, further research is needed to assess the ecological significance of these opportunistic macroalgal blooms in the Yellow Sea ecosystem.

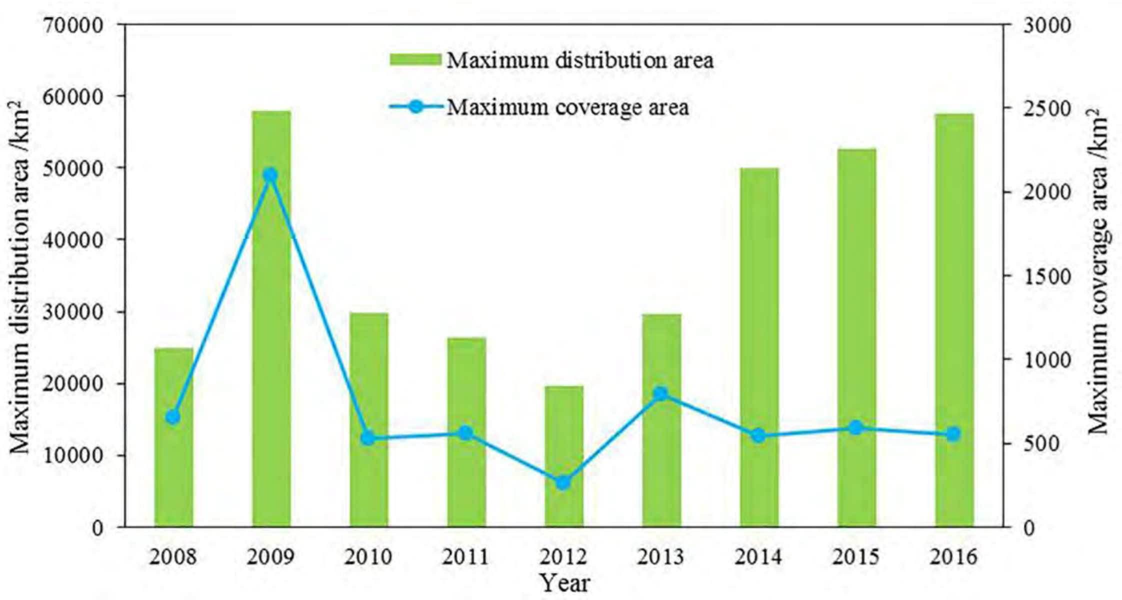

Figure R20-21. Maximum distribution area and coverage area of green tides in the Yellow Sea during 2008-2016 (data from the State Oceanic Administration, People's Republic of China, http://www.soa.gov.cn).

6 Zooplankton

6.1 Mesozooplankton

In the Yellow Sea, copepods account for 70-90% of the zooplankton abundance but there were seasonal and areal variations (Kang and Lee 1991; Rebstock and Kang 2003). Among the copepods, *Calanus sinicus, Paracalanus* sp., *Oithona atlantica*, and *Corycaeus affinis* were dominant through all seasons and occurred in most areas, comprising 75.6% of the total copepod biomass. Apart from copepods, *Sagitta crassa, Euphausia pacifica* were also dominant (Tang 1989). Oceanic, warm water species were rare but found episodically in the Yellow Sea.

In the Korean waters including the eastern Yellow Sea, a small seasonal peak in the zooplankton biomass occurred in autumn (Kang and Ohman 2014). Seasonal variation of zooplankton biomass was generally low in winter (February and December) and high in late spring-autumn (June-October). Kang (2008) reported that zooplankton biomass showed seasonal peaks in the June and October in the eastern Yellow Sea. Bimonthly mean abundance of four zooplankton groups, copepods, euphausiids, amphipods and chaetognaths showed seasonal variations. Abundance of copepods, euphausiids and amphipods were highest in June, while chaetognaths abundance was highest in August.

There is some evidence of decadal long-term changes in the eastern Yellow Sea. Zooplankton biomass showed a gradual increase with some fluctuations (Figure R20-22a). Biomass remarkably increased from the mid-1980s to the early 1990s. After the early 2000s, biomass increased continuously until 2010. The increasing zooplankton biomass was closely associated with increases of all four major zooplankton groups (copepods, chaetognaths, euphausiids, and amphipods) (Kang and Ohman 2014). Annual mean abundance of four zooplankton groups (copepods, chaetognaths, amphipods and euphausiids) in the eastern Yellow Sea showed a similar trend among copepods and chaetognaths after the mid-1990s, while amphipods and euphausiids showed no typical trends (Figure R20-23).

The patterns in the annual anomalies of copepods and chaetognaths were out of phase before the mid-1990s but shifted in phase after the mid-1990s (Figure R20-24). They showed the positive values continuously after the mid-2000s. Amphipods also showed positive values after the mid-2000s except for 2014. In contrast to copepods, chaetognaths and amphipods, the anomalies of euphausiid abundance showed positive values in the late 1970s and the early 1980s and shifted to negative values.

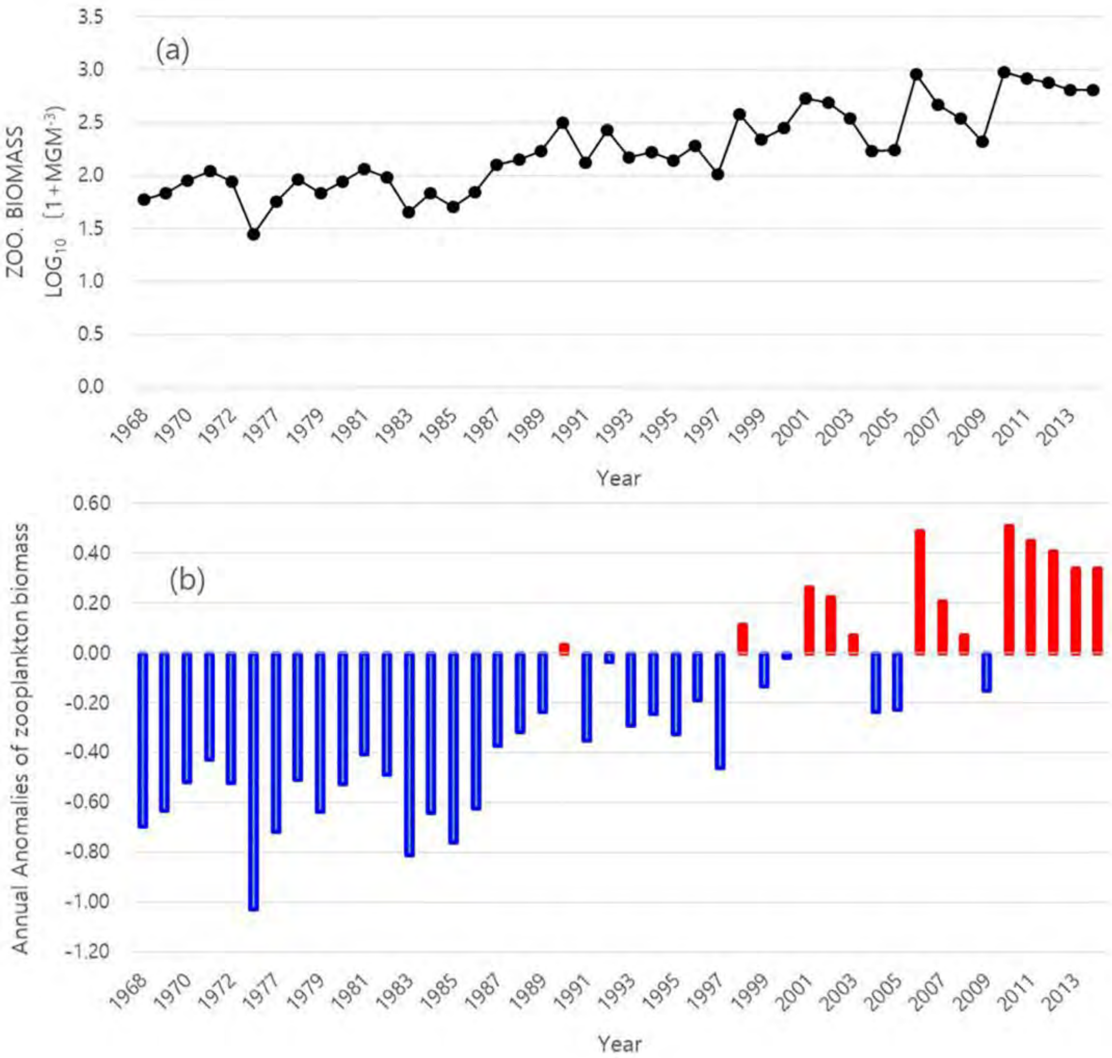

Figure R20-22. Time series of annual mean of zooplankton biomass (log_{10}-transformed) (a) and their anomalies (b) in the eastern Yellow Sea.

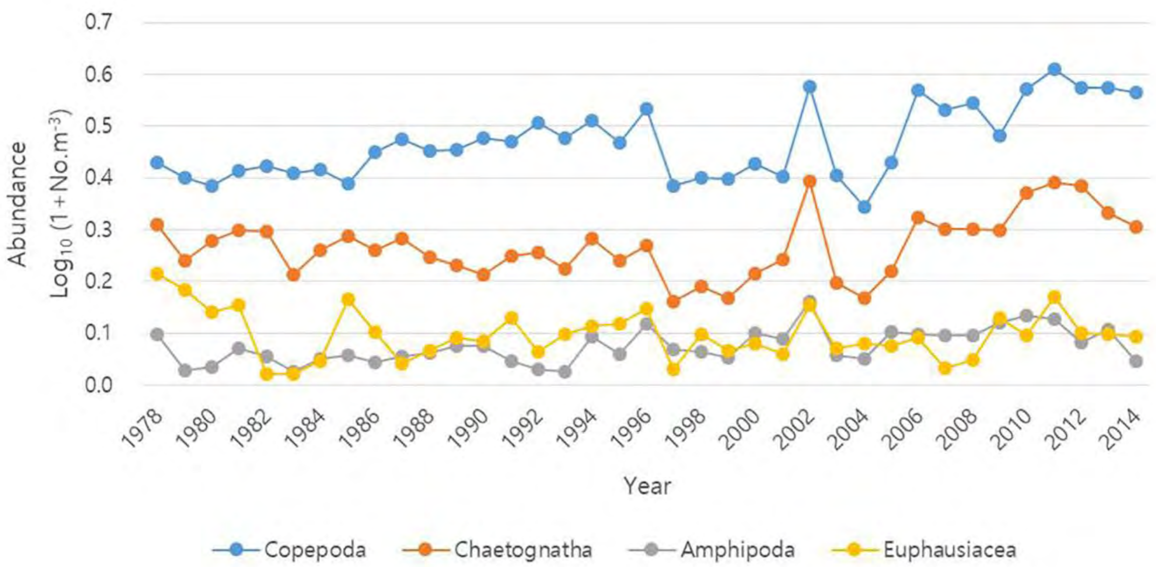

Figure R20-23. Time series of annual mean of zooplankton biomass ($\log_{10}$-transformed) in the eastern Yellow Sea.

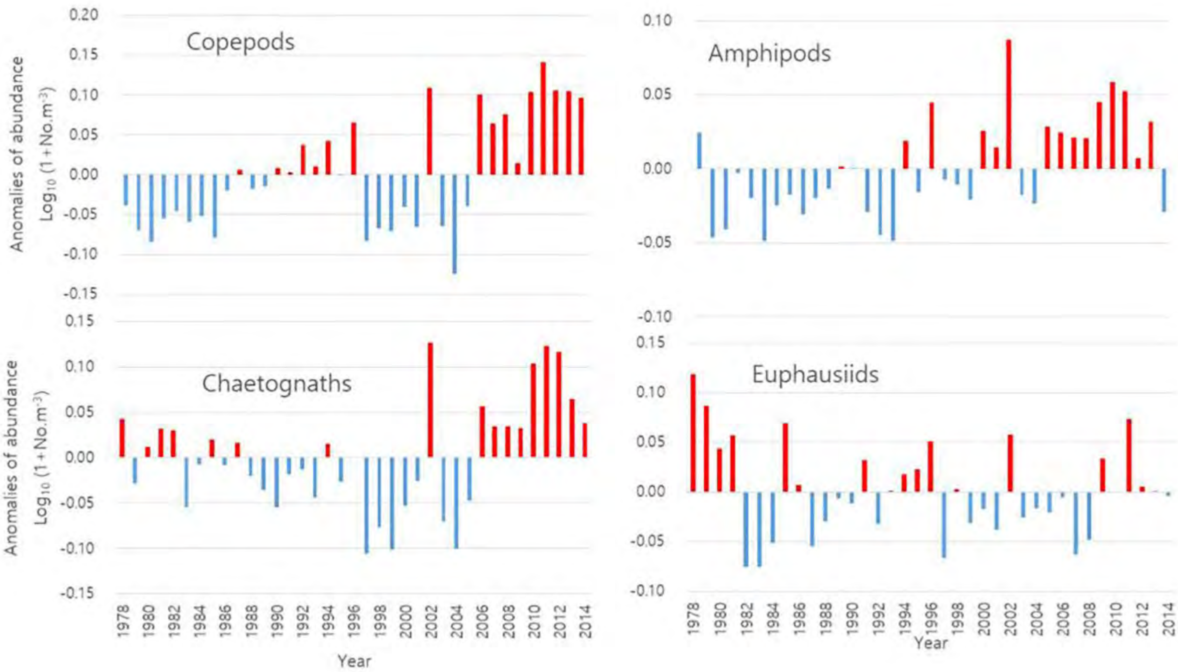

Figure R20-24. Anomalies of annual mean of zooplankton biomass ($\log_{10}$-transformed) in the eastern Yellow Sea.

In contrast to the increasing trend in the eastern Yellow Sea, a decreasing trend in the total zooplankton abundance was observed at a coastal station (near the Jiaozhou Bay: 35°59′00″N, 120°25′30″E) in the western Yellow Sea. Four season data for mesozooplankton from 2003 to 2013 were obtained as a part of a long-term research program. During the 11-year sampling, total zooplankton abundance showed a decreasing trend with its peak value in August 2005 (Figure R20-25). According to the time series change of zooplankton abundance in different seasons, the overall decrease in zooplankton abundance can be attributed to the decline in spring, summer and autumn (Figure R20-26). Seasonal variation of zooplankton abundance was generally lowest in autumn (November) and highest in late spring/summer (May-August).

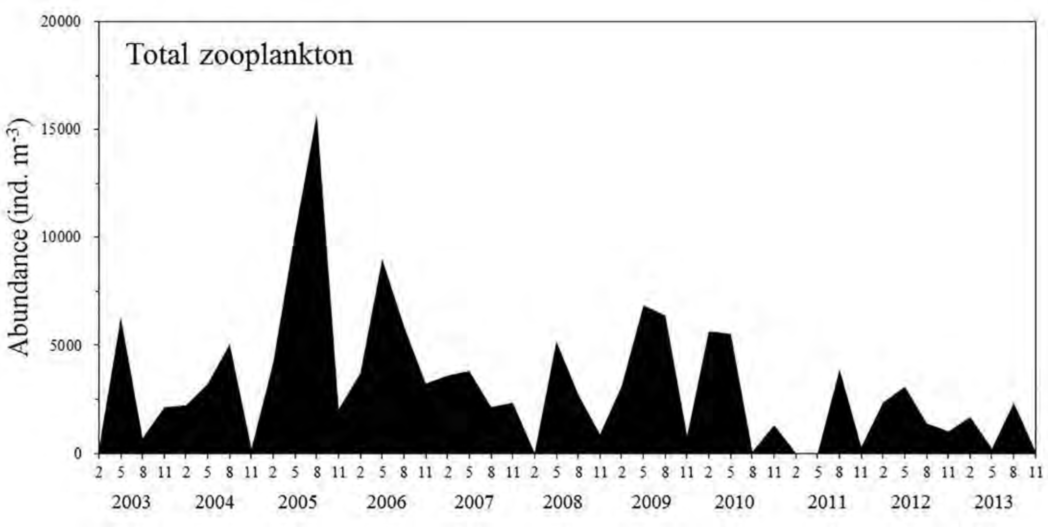

Figure R20-25. Time series of quarterly zooplankton abundance (ind. m^{-3}) in the western Yellow Sea during 2003-2013.

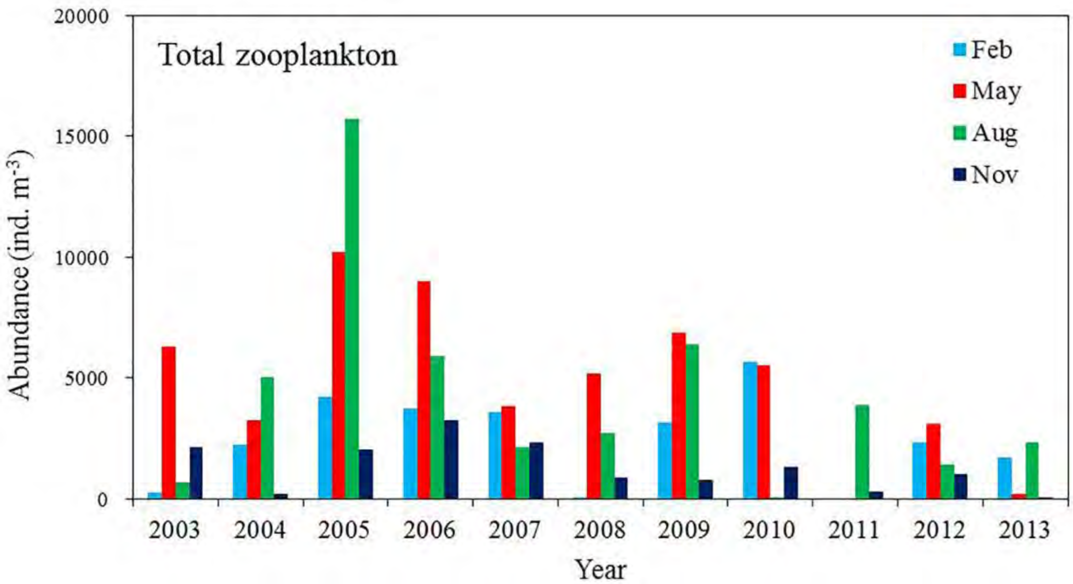

Figure R20-26. Time series of zooplankton abundance (ind. m^{-3}) in different seasons in the western Yellow Sea during 2003-2013.

6.2 Gelatinous zooplankton

A conspicuous feature of the zooplankton community in the region in recent years is the blooms of the large scyphomedusa, *Nemopilema nomurai* (giant jellyfish) (Anonymous 2004). An unusual bloom was first observed in 2000 with large blooms occurring in 2003. Ocean currents carried the jellyfish blooms northward into the adjacent seas causing serious problems for fishermen (and beach bathers). The jellyfish observed in Korean waters includes the giant *Nemopilema nomurai*, medium-sized *Aurelia aurita*, big and venomous *Cyanea capillata* and *Dactylometra quinquecirrha* (*Chrysaora quinquecirrha*). Highly venomous *Physalia physalis* and *Carybdea rastonii* are also reported occasionally. *N. nomurai* is the biggest jellyfish occurring in Korean waters with a bell size of about 2 m and weight of 150 kg. Outbreaks of these were reported by Japanese fishermen in 1920, 1958, 1995, and 2002. The causes of the blooms and their interannual fluctuation are unknown. Several factors such as increasing sea temperature, overfishing, and marine pollution have been suggested as causal factors or at least mediators.

The giant jellyfish have occurred in the region in large numbers since 2003. From the monitoring surveys at 52 stations every August in the Yellow Sea (Figure R20-27), the abundance of *N. nomurai* was highest in 2005 (103.03 indiv. ha^{-1}), followed by 2006 and 2007 (Figure R20-27). Since 2008, it has been extremely low and in 2017, no individual was detected.

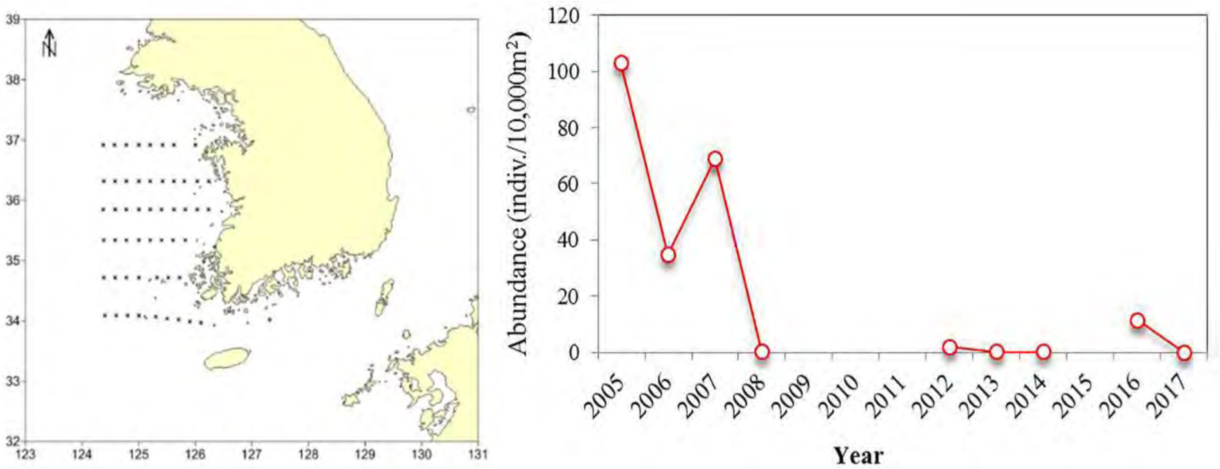

Figure R20-27. Jellyfish monitoring sites in Yellow Sea on Korean Series of Oceanographic Monitoring Program (Left). Interannual variation of the abundance of *Nemopilema nomurai* in Yellow Sea in 2005-2017 (right).

A different trend was observed at a coastal station (near the Jiaozhou Bay: 35°59′00″N, 120°25′30″E) in the western Yellow Sea. During the 11-year sampling, medusae abundance showed a drastic fluctuation with its peak value in May 2009 (Figure R20-28). According to the time series change of medusae abundance in different seasons, the abundance of medusae presented an increasing trend in spring (Figure R20-29). There were three conspicuous maxima in May of 2007, 2009 and 2012. Seasonal variation of medusa abundance was generally lowest in autumn (November) and highest in late spring/summer (May-August).

The increasing trend of small jellyfish has also been recorded in the recent decade in Jiaozhou Bay, which was a eutrophic semi-enclosed bay in the western part of the Yellow Sea, China (Sun et al. 2012). In addition, the biodiversity of jellyfish has also increased significantly in recent years with a change in dominant species. The changes in small jellyfish abundance and species composition seemed related to both climate change (e.g. warming) and human activities (e.g. eutrophication, aquaculture and coastal construction activities around the bay).

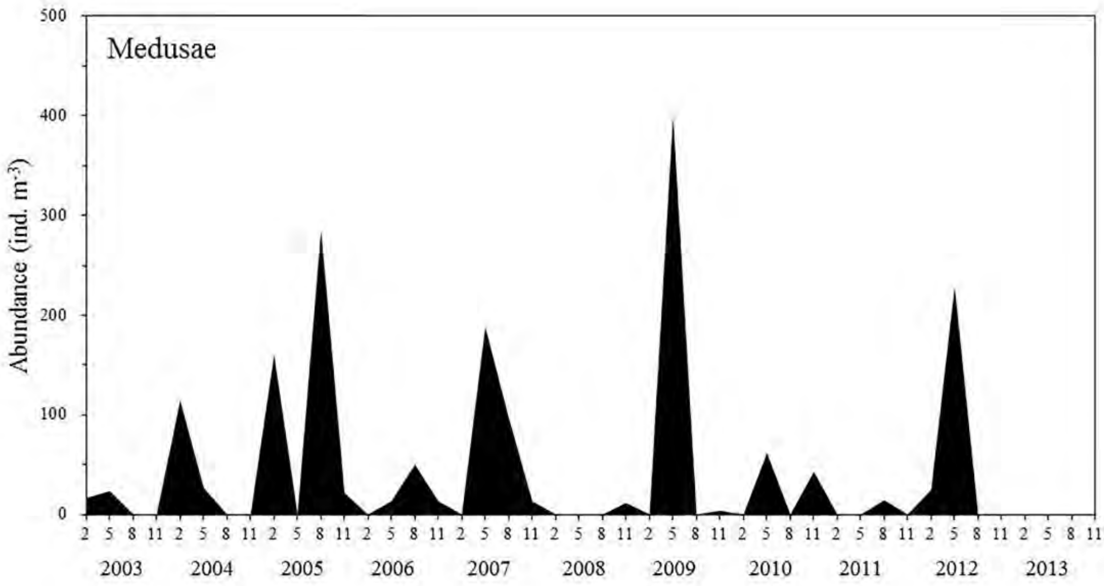

Figure R20-28. Time series of quarterly medusae abundance (ind. m^{-3}) in the western Yellow Sea during 2003-2013.

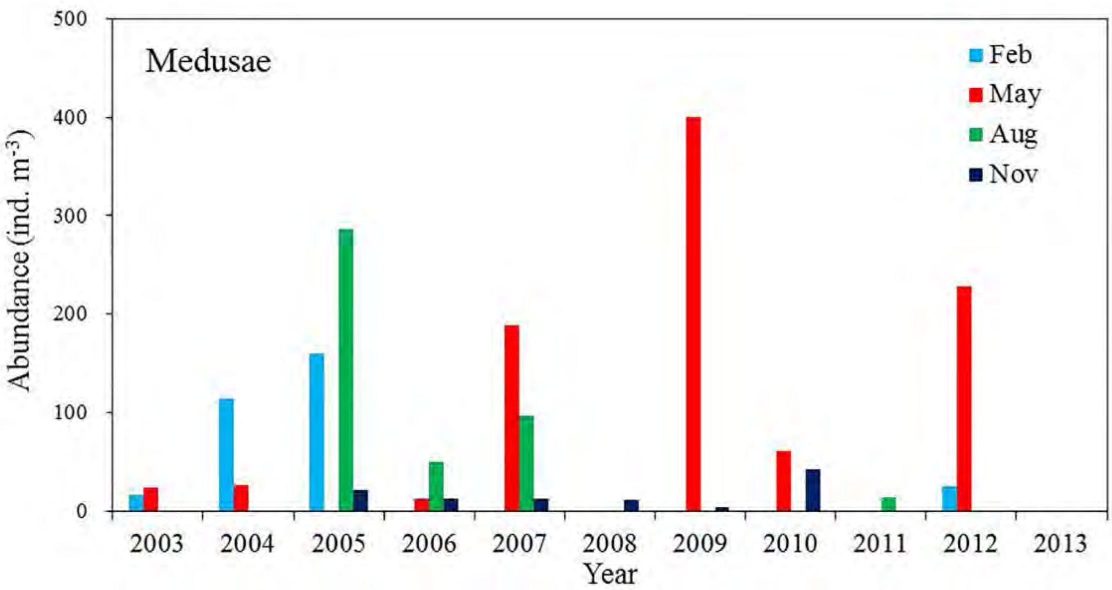

Figure R20-29. Time series of medusae abundance (ind. m^{-3}) in different seasons in the western Yellow Sea during 2003-2013.

7 Fishes and Invertebrates

7.1 Species Composition/Diversity

A total of 339 fish species belonging to 219 genera and 109 families were reported and compiled on the Korean side of the Yellow Sea (Lee 2004). While the winter bottom trawl surveys (mesh size = 24 mm) conducted by the Yellow Sea Fisheries Research Institute in the Chinese waters of the Yellow Sea from 2003 to 2015 listed 42 species (Chen et al. 2017), the summer surveys (mesh size = 20 mm) conducted by the National Institute of Fisheries Science of Korea in the deep, middle part of the Yellow Sea from 2008 to 2014 reported to have sampled 72 demersal fish species (Koh et al. 2016). The diversity indices and the size spectra of fish assemblages generally did not reveal any clear trend from 2003 to 2015, but the dominance of the relatively small species, anchovy, tended to have decreased (Chen et al. 2017). The 5 most dominant fish species in biomass in the Chinese winter bottom trawl surveys were anchovy (*Engraulis japonicus*), angler fish (*Lophius litulon*), small yellow croaker (*Larimichthys polyactis*), silver pomfret (*Pampus argenteus*) and Tanaka's snailfish (*Liparis tanakae*); whereas they were Tanaka's snailfish, small yellow croaker, angler fish, anchovy and Pacific cod (*Gadus microcephalus*) in the Korean summer surveys.

Among 84 fish and invertebrate species reported with species names in the Yellow Sea from 1950 to 2014, the dominant species in catch biomass were largehead hairtail (*Trichiurus lepturus*), chub mackerel (*Scomber japonicus*), and anchovy, followed by Pacific saury (*Cololabis saira*), akiami paste shrimp (*Acetes japonicas*), small yellow croaker, blue crab (*Portunus trituberculatus*), Pacific sardine (*Sardinops sagax*), yellow striped flounder (*Pseudopleuronectes herzensteini*), Pacific herring (*Clupea pallasii pallasii*) and southern rough shrimp (*Trachysalambria curvirostris*) (Figure R20-30).

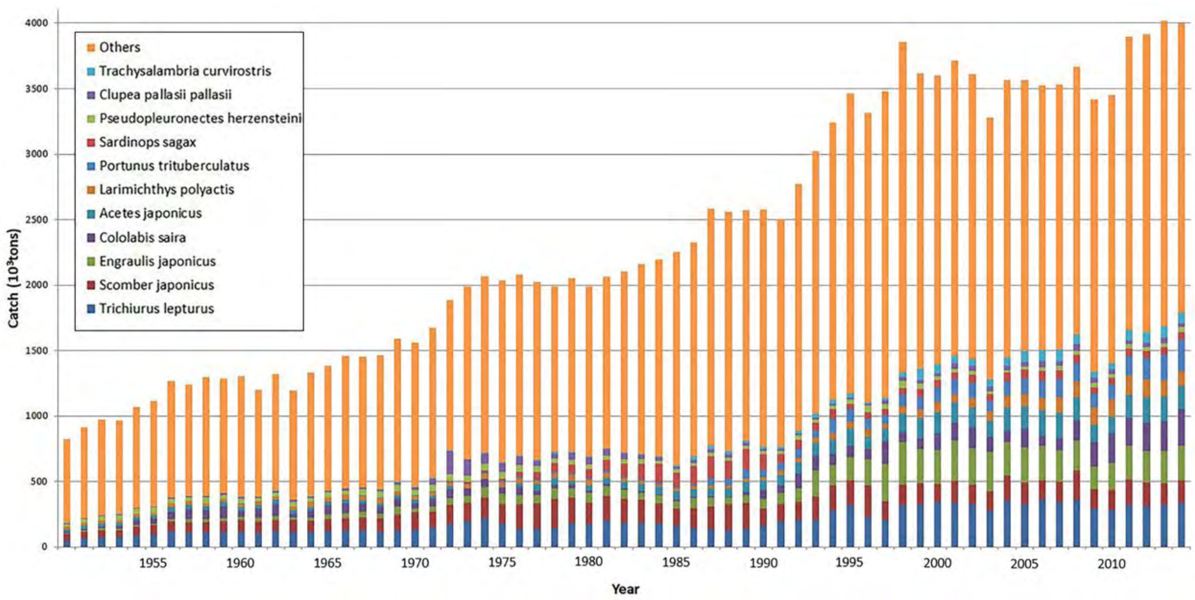

Figure R20-30. Annual commercial catch by species in the Yellow Sea from 1950 to 2014.

Correspondence analysis on species composition of annual commercial catch suggested that the fish community structure has changed gradually, and the entire period can be divided into the following 4 distinct regimes: 1) 1950-1976, 2) 1977-1989, 3) 1990-1998, and 4) 1999-2014 (Figure R20-31). These 4 regimes generally match with the reported regime shifts in the North Pacific by past studies (Hare and Mantua 2000; Zhang et al. 2000; Zhang et al. 2004; Katoh et al. 2006; Tian et al. 2008; Hwang and Jung 2012; Jung 2014). The species whose biomass composition was relatively dominant in the first regime (1950-1976) compared with the other periods include slender rainbow sardine (*Dussumieria elopsoides*), imposter trevally (*Carangoides talamparoides*), sandfish (*Arctoscopus japonicus*), olive flounder (*Paralichthys olivaceus*), Pacific red gurnard (*Chelidonichthys kumu*) and small yellow croaker. Those species in the second regime (1977-1989) are represented by giant tiger prawn (*Penaeus monodon*), blackmouth croaker (*Atrobucca nibe*), yellowfin tuna (*Thunnus albacares*), silver pomfret (*Pampus argenteus*) and black pompfret (*Parastromateus niger*). During the third regime (1990-1998), the species composition had gradually shifted from the first to the fourth regime, and the characteristic species were *Sardinella zunasi*, sardine (*Sardinops sagax*), bigeye tuna (*Thunnus obesus*) and atka mackerel (*Pleurogrammus azonus*). Finally, the fourth regime (1990-2014) was featured by flower crab (*Portunus pelagicus*), blue crab (*Portunus trituberculatus*), daggertooth pike conger (*Muraenesox cinereus*), flathead grey mullet (*Mugil cephalus*), *Trachysalambria curvirostris*, red seabream (*Pagrus major*), and slender shad (*Ilisha elongate*).

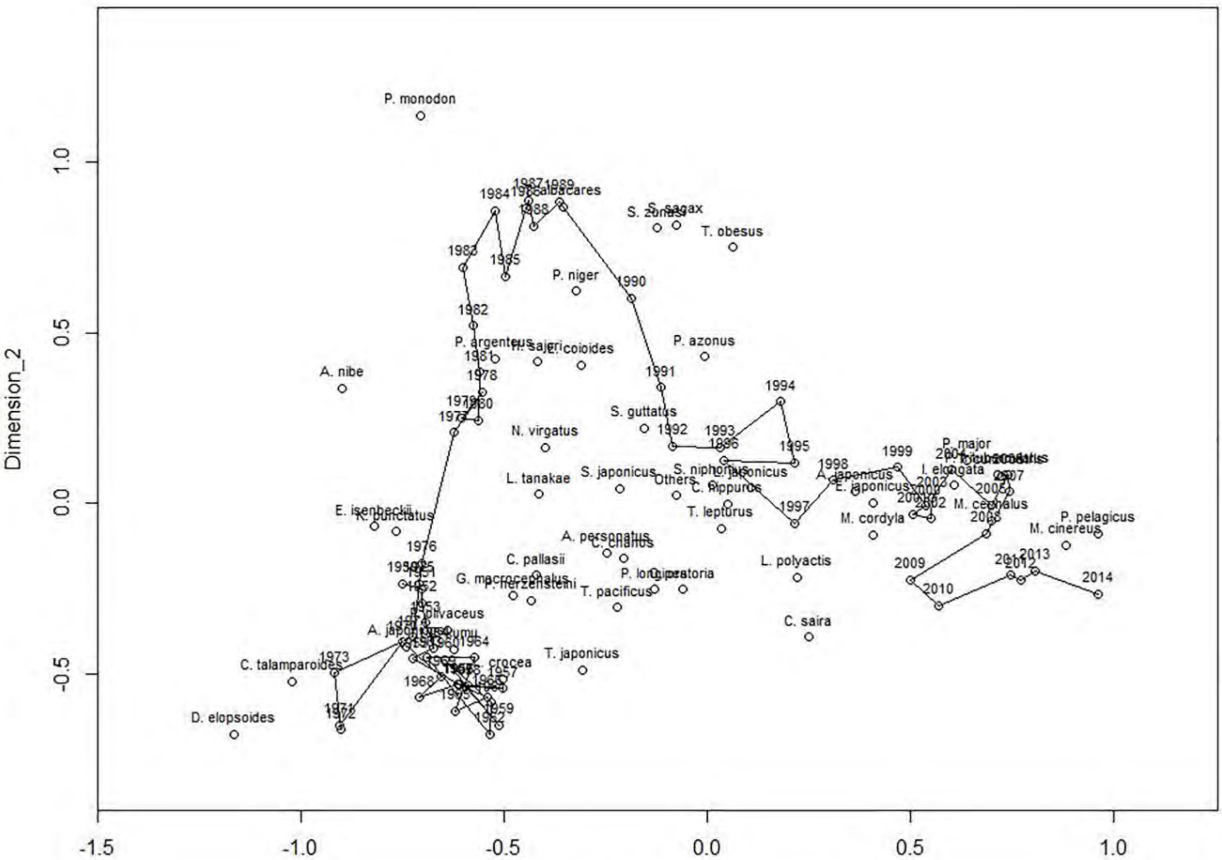

Figure R20-31. Correspondence analysis of species composition in commercial catch in the Yellow Sea from 1950 to 2014. The catch data were based on the official national reports compiled by Food and Agricultural Organization of the United Nations and adjusted for the unreported catch by Sea Around Us (Sea Around Us 2017).

7.2 Catch and Biomass

A total of 186 taxonomic groups including a total of 84 fish and invertebrate species have been reported as exploited from 1950 to 2014 (Sea Around Us 2017). Annual commercial catch has steadily increased from ca. 0.8 x 10^6 tons in 1950 to ca. 4.0 x 10^6 tons in 2014 (Sea Around Us 2017) (Figure R20-30). By nation, during the period of 2008-2014, China accounted for most of the annual catch (ca. 80%), followed by South Korea (14%), Hong Kong (4%), and North Korea (2%). The dominant taxonomic groups during this period were Scyphozoa, largehead hairtail, anchovy, saury, chub mackerel, akiami paste shrimp, blue crab, small yellow croaker and Pampus (Figure R20-32). Possibly due to overexploitation, the mean individual weight and the catch-per-unit-effort of an individual species were twice more likely to show a decreasing trend than to show an increasing trend (Chen et al. 2017).

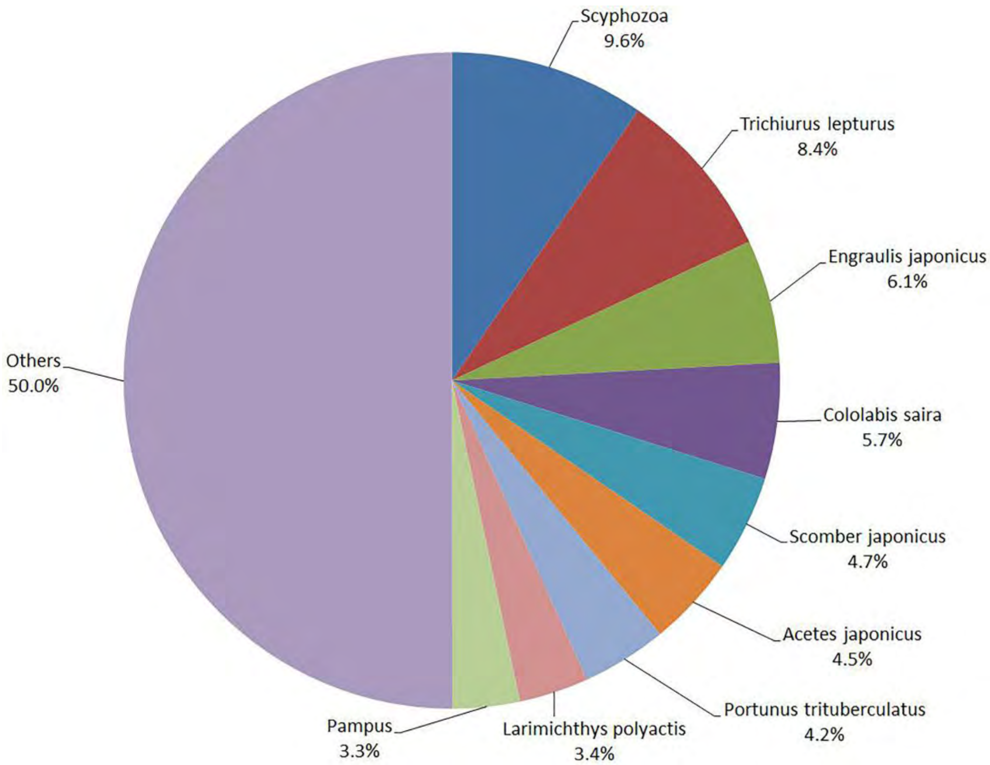

Figure R20-32. The dominant taxonomic groups in the recent commercial fisheries catches in the Yellow Sea from 2008 to 2014.

7.3 Distribution

Among the 9 major commercial fish species exploited by Korean fishers, 5 species (horse mackerel, Pacific sardine, common squid, Spanish mackerel and yellowtail) showed significant northward shifts in catch distribution, but one species (anchovy) showed a southward shift in relation with seawater warming (Jung et al. 2014). The estimated distance of northward shift in the mean latitude of catch was especially greater for Spanish mackerel and yellowtail. Despite no significant correlation with depth-specific water temperatures, the two dominant species of the Yellow Sea, largehead hairtail and yellow croaker, did show a long-term (1985-2010) northward shift in their catch distribution (Jung et al. 2014).

7.4 Recruitment

The stock size of anchovy was estimated to have declined by overfishing since 1996 (Zhao et al. 2003), and tentatively projected to may decline due to global warming and the subsequent confinement of cold water masses within the Yellow Sea (Jung et al. 2016). The average body size and age of small yellow croaker (*Larimichthys polyactis*) had decreased from 1985 to 2008, which was attributed mainly to the increased fishing activity (Shan et al. 2017).

8 Macrozoobenthos in the Yellow Sea

8.1 Assemblages

A comprehensive review by Liu (2013) indicated a total of 22,629 marine species have been recorded in the China seas since 1950s, indicating one of global hotspots for marine biodiversity in the world. In the macrozoobenthos, 1,987 species were found in the Bohai and Yellow seas. Species composition in Bohai and Yellow seas indicated the greatest proportion of the phylum Mollusca (n=981; 49%) followed by Arthropoda (n=409; 21%), Annelida (n=367; 18%), Bryozoa (n=116; 6%), Echinodermata (n=54; 3%), Cnidaria (n=50; 2.5%), and Porifera (n=10; 0.5%) (Figure R20-33). In general, mollusk and arthropod species prevailed.

A recent review by Park et al. (2014) updated the list of macrozoobenthos in Korean coastal areas, targeting intertidal and subtidal zones in the eastern Yellow Sea. This study compiled a total of 72 peer-reviewed articles relating to the taxonomy and ecology of macrozoobenthos reported since 1970s and listed a total of 624 species belonging to 10 phyla. Species composition indicated the dominance of the phylum Annelida (n=248, 40%) followed by Mollusca (n=196, 31%), Arthropoda (n=135, 22%), Echinodermata (n=16; 2.6%), Cnidaria (n=14; 2.4%), and others (n=14, 2.2%) (Figure R20-33). While annelids species prevailed in the subtidal zone, mollusk and arthropod species did in the intertidal area. An apparent difference on phylum and species compositions between China and Korea could be expected from the discrepancy in meta-data set (namely, coverage areas), i.e., the macrozoobenthos meta-data for the Korean coastal areas did not cover the open sea area of the Yellow Sea at this time. Nevertheless, the 624 species of macrozoobenthos found in the Korean tidal flats indicates a significantly high species diversity in the given area, ~2500 km^2 of tidal flats (Koh and Khim 2014).

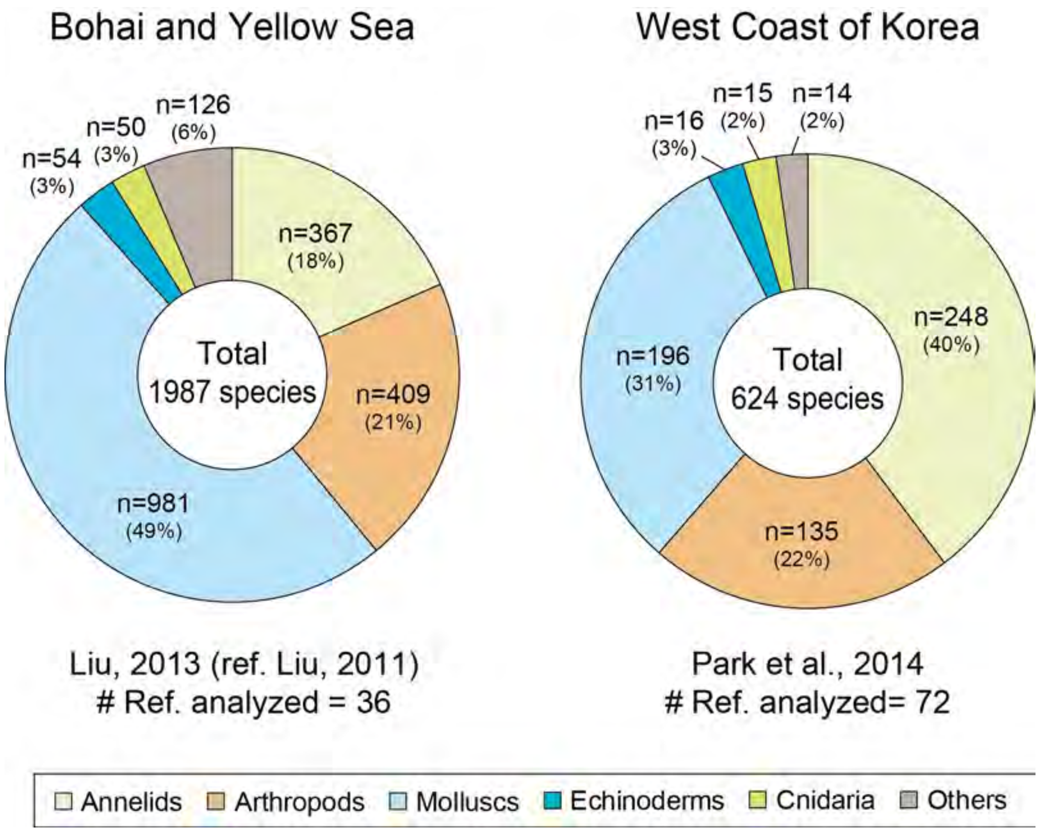

Figure R20-33. Macrozoobenthos recorded in the Bohai and Yellow seas (left) and in the west coast of Korea (right), showing the species composition at phylum level; data analyzed from 2 key review papers for China (Liu 2011) and Korea (Park et al. 2014), where 36 and 72 peer-reviewed articles were compiled, respectively.

8.2 Temporal changes

Due to the lack of systematic ecological monitoring for the marine life in the Yellow Sea both in China (Liu 2013) and Korea (Koh and Khim 2014), particularly for the macrozoobenthos, it is quite difficult to adequately address the long-term changes in the species assemblage and distribution of macrozoobenthos. With limited data, the temporal changes in species composition, abundance and biomass are examined for the Yellow Sea macrozoobenthos (Figure R20-34). The macrofaunal species composition at phylum level in the mid-Yellow Sea did not seem to greatly change during the past 30 years at an inter-decadal scale (Figure R20-34a), with lesser proportional variations cross the phylum. Not surprisingly, the phylum Annelida was found to be a dominant taxon in the open sea area of the Yellow Sea, contributing about half of the total species (mean=46%) since 1990s until present. Arthropods (mean=23%) and Molluscs (mean=19%) were collectively the next two dominant taxa, explaining about the remaining half of the macrozoobenthos assemblage.

Meantime, the density and biomass of the macrozoobenthos much varied at inter-decadal period (Figure R20-34c), for example total density was greatest in 2000s compared to that in 1990s and 2010s, which was explained by a drastic increase of Arthropods abundance. It was noteworthy that the addition of newly recorded crustacean species reached 452 in the Yellow Sea during the years of 2002-2006, which might explain such rapid increase of abundance. The biomass of macrozoobenthos showed an inter-decadal increase, which paralleled a similar increase of echinoderms species. Finally, the ecological indices, such as

Shannon-Wiener (H') and species richness (d) suggest a slight ecological deterioration in 2010s compared to previous periods, but such changes may not be significant considering the narrow range and/or small variations across the data-sets (Figure R20-34d). Overall, the macrozoobenthos assemblages and distributions in the Yellow Sea indicate that the ecosystem has a diverse benthic invertebrate fauna in the world, particularly in terms of species richness per area (Costello et al. 2010).

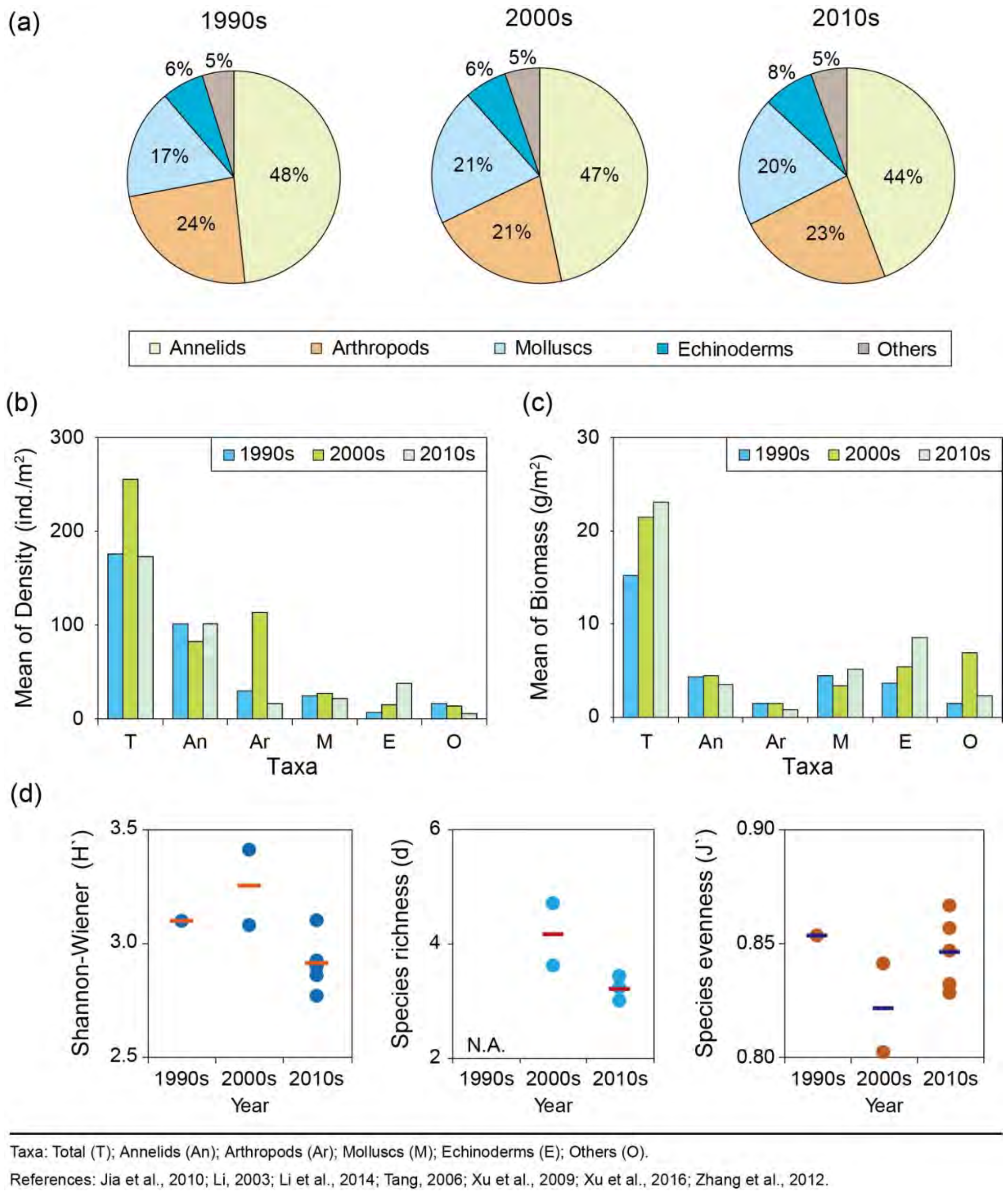

Figure R20-34. Long-term changes in macrozoobenthos assemblages in the mid Yellow Sea, showing (a) species composition at phylum level, (b) species abundance, (c) biomass, and (d) ecological quality indices; data analyzed from 7 peer-reviewed articles.

9 Marine birds

The intertidal areas and coastal wetlands of the Yellow Sea support more than 2 million shorebirds during their northward migration; about 40% of the all migratory shorebirds in the East Asian-Australasian Flyway (Barter 2002). A number of shorebird species have been found to occur in internationally important numbers at one or more sites in the Yellow Sea, representing 60% of the migratory shorebird species occurring in the flyway. Two of the species are classified as globally threatened, the Nordmann's greenshank (*Tringa guttifer*) and the spoon-billed sandpiper (*Calidris pygmaea),* whilst two are near-threatened, the eastern curlew (*Numenius madagascariensis*) and Asian dowitcher (*Limnodromus semipalmatus*). While the South Korean coastline has been well surveyed, only about one-third of the Chinese coasts have been surveyed and little is known from North Korea.

Over 60 species of seabirds and shorebirds have been recorded in the Korean shores of the Yellow Sea. A total of 44 species and over 144,962 individuals of shorebirds including 5 endangered species visited in spring and autumn (National Institute of Biological Resources, here after NIBR, 2015a). The total number of shorebirds in the Yellow Sea was 34,709-144,962 individuals in 2015 (Figure R20-35). Among them, Nordmann's greenshank (*Tringa guttifer*), red knot (*Calidris tenuirostris*), far eastern curlew *(Numernius madagascariensis*) and black-faced spoonbill (*Platalea minor*) are listed as endangered species on the IUCN Red List. Spoon-billed sandpiper (*Calidris pygmaea*) which is critically endangered species on the IUCN Red List was also observed. The Yellow Sea is important to breeding seabirds as well.

More than 10 species of seabirds breed in remote islands of the Yellow Sea. 90% of world population of Swinhoe's storm-petrel (*Coceanodroma monorhis*) breeds in the five islands. The breeding population of Swinhoe's storm-petrels was 9,000-13,000 pairs on the Chilbaldo Island (Korea National Park Research Institute 2014). It has significantly declined by 39-55% since 1986 (Lee et al. 2012). The main threat was the entanglement by introduced plants on the breeding sites. The breeding population of streaked shearwaters (*Calonectris leucomelas*) was stable (15,000-16000 pairs) on the Sasudo Island. However, less than half of their eggs successfully fledged (Nam and Yoo 2017) because of the predation by introduced rats (*Rattus norvegicus*) (Nam et al. 2014). Although local people used seabirds or their eggs as food in the past, many of their breeding colonies are now protected as the Marine National Parks, Protected Areas or National Monuments under the law. The breeding population of black-tailed gull (*Larus crassirostris*) is stable on the Hongdo Island (Figure R20-36). Crested murrelet (*Synthliboramphus wumizusume*) and ancient murrelet (*S. antiques*) also breed on several islands. Breeding population of these two murrelets was estimated as 249-2,303 pairs on the Guguldo Island (Park 2013). Every year, seabirds visited to spend winter in the Yellow Sea. Over 10,000 individuals of Saunder's gulls (*Saundersilarus saundersi*) spent winters in the Korean coasts in the Yellow Sea (NIBR 2008, 2009, 2010b, 2011b, 2012b, 2013b, 2014b, 2015b, 2016). The wintering population of Saunder's Gulls tends to increase between 2008 and 2016 (Figure R20-37).

The main threats to seabirds are introduced plants and animals such as rats and feral cats, habitat loss and bycatch in the Yellow Sea. Climate change impacts such as rising of sea level and seawater temperature are also potential threats to the seabirds and shorebirds.

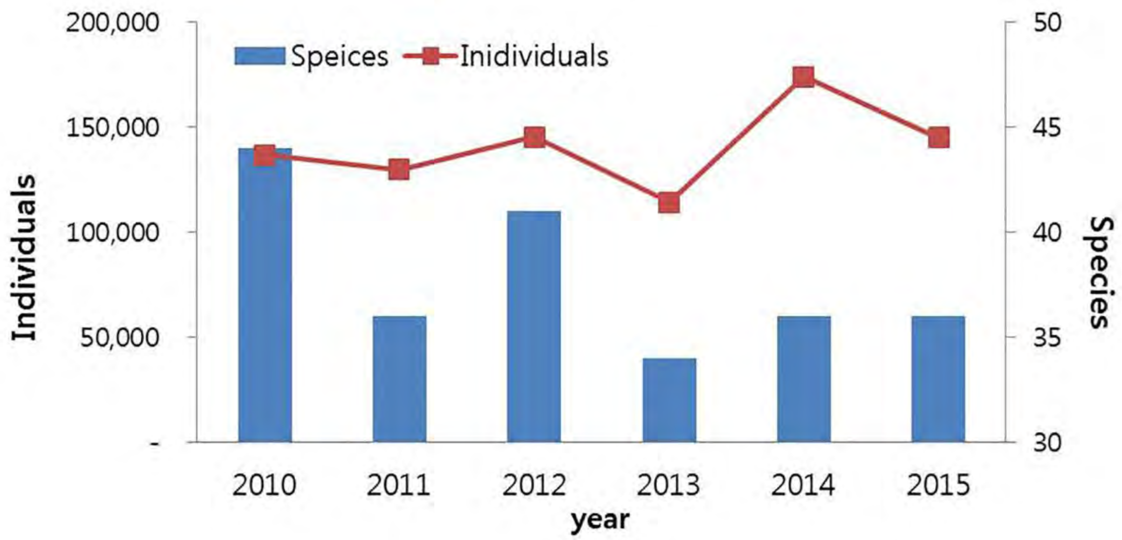

Figure R20-35. Shorebirds survey from 2010 to 2015 (NIBR 2010a, 2011a, 2012a, 2013a, 2014a, 2015a)

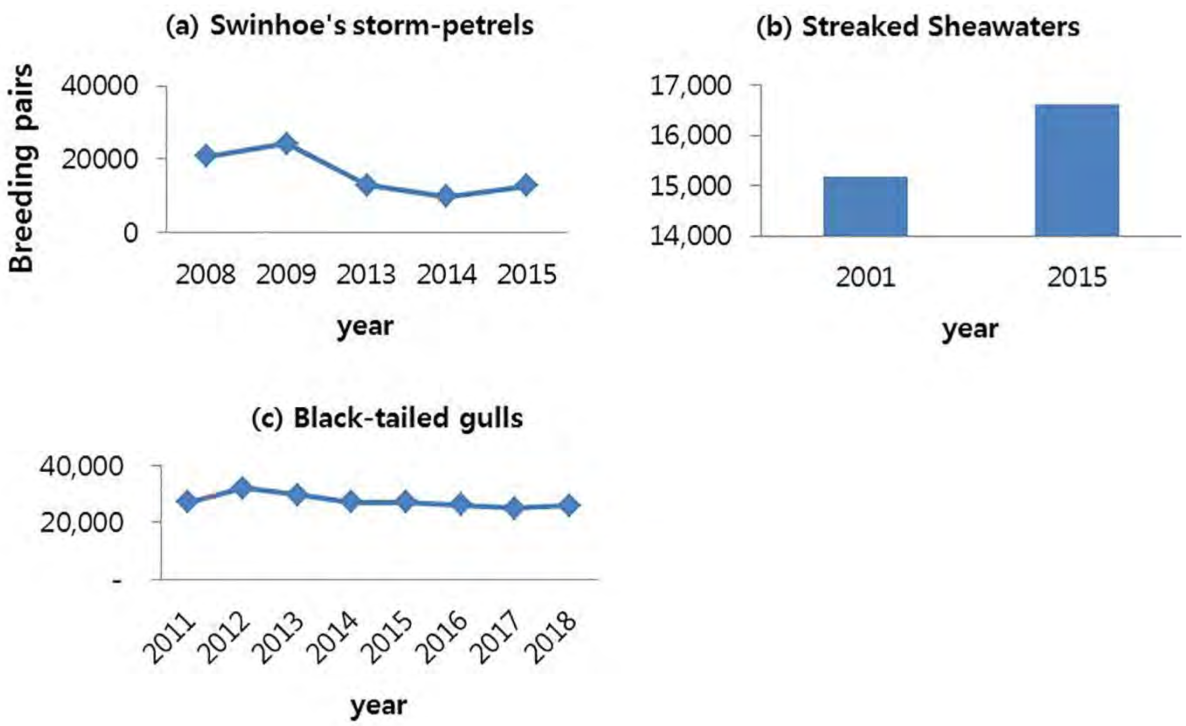

Figure R20-36. Breeding population of (a) the Swinhoe's storm-petrel on Chilbaldo Island (Kang et al. 2008; Korea National Park Research Institute, 2014 and 2015), (b) the streaked shearwater on Sasudo Island (Nam and Yoo 2017), and (c) the black-tailed Gull on Hongdo Island, Gyungnam (Korea National Park Research Institute 2018).

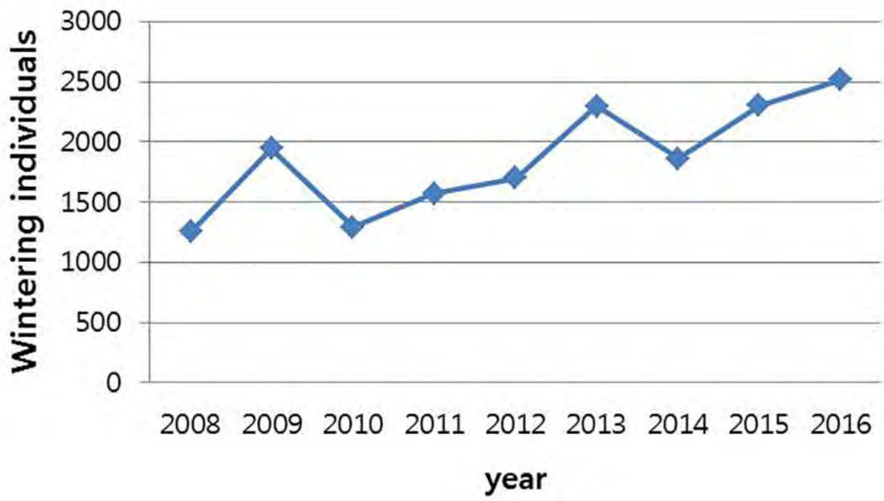

Figure R20-37. Wintering population of the Saunders gull (NIBR 2008, 2009, 2010, 2011, 2012, 2013, 2014, 2015, 2016)

10 Marine mammals

10.1 Pinnipeds

Spotted Seals (*Phoca largha)*, the only pinniped that regularly inhabit in the Yellow Sea, are designated as protected animals in both Korea and China and hunting them has been banned since early 1980s (Won and Yoo 2004). The population size of spotted seals in the Yellow Sea was about 8,000 individuals in 1940 (Dong and Shen 1991). Since the 1960s, populations have been decreasing due to heavy catch and habitat destruction and only small groups can now be found. They breed in Liaodong Bay, China in winter season. The major haul-out sites are on the Baengnyeong-do, South Korea, where 200-400 individuals regularly stay between spring to fall. Abundance of the population in the Liaodong Bay is assumed around 1,200 individuals (Han 2018). Since 2000, counting surveys of spotted seals have conducted on the haul-out sites of the Baengnyeong-do. A maximum of 343 individuals was observed in 2002. Recently, the number of spotted seals has decreased from the early 2000s (Figure R20-38). Whether this indicates a reduction in the population size is not clear. In 2017, 190 individuals of the seal were counted, whereas 410 individuals were photo-identified at the same year using unique spot patterns on their chick pelages as natural marker (Cetacean Research Institute, NIFS, 2018).

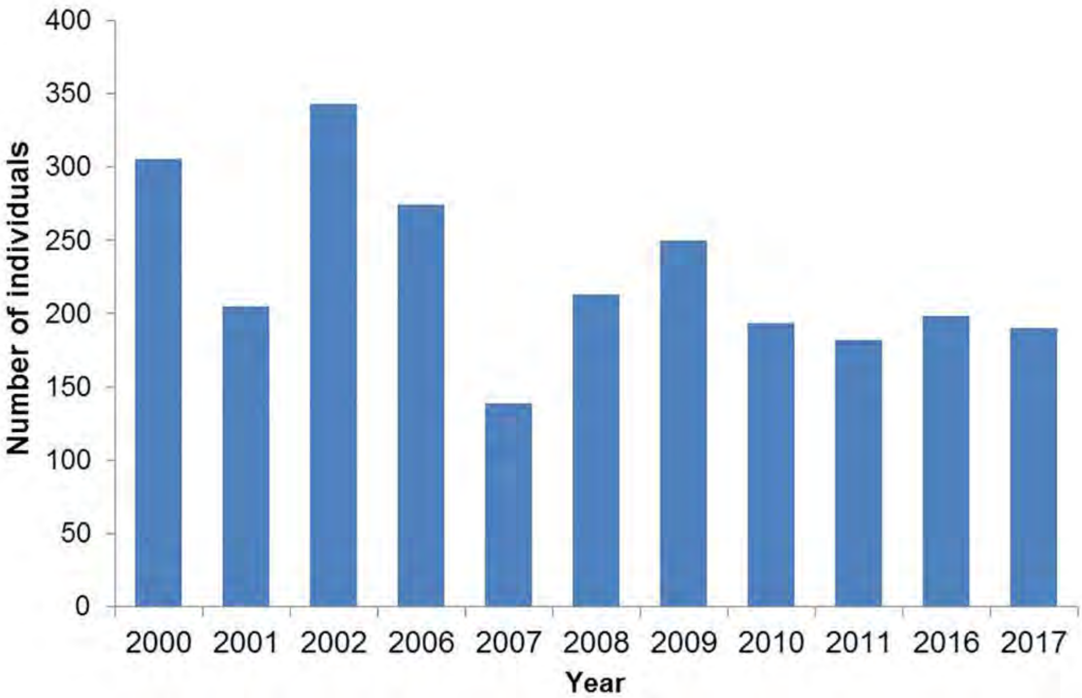

Figure R20-38. Census of spotted seals (*Phoca largha*) around Baengnyeong-do between 2000 and 2017.

10.2 Cetaceans

A total of 16 cetacean species have been recorded. Amongst them, fin whale (*Balaenoptera physalus*), minke whale (*B. acutrostrata*), killer whale (*Orcinus orca*), Blainville's beaked whale (*Mesoplodon densirostris*), and finless porpoise (*Neophocaena phocaenoides*) have commonly been observed. Catching whales was banned in Korea in 1986 and some of the whale populations have increased. In the Changjiang River estuary and Yangtze River, two endangered migratory freshwater cetaceans can be found, baiji (*Lipotes vexillifer*) and finless porpoise. The former, listed as a critically endangered species in IUCN Red List, lives only in China (The Yellow Sea Ecoregion Initiative 2001) In Korean waters, finless porpoises are typically observed in nearshore areas while minke whales are observed in offshore areas. Surveys in Korean coastal waters of the Yellow Sea show that the number of minke whales was reduced from 1,685 in 2001 to 733 in 2008, although this may not be statistically significant.

Finless porpoise is the most abundant species in the Yellow Sea. However, they have decreased by approximately 70% between 2004/2005 and 2011 (Park et al. 2015). The abundance estimates of the finless porpoise in the Korean coastal waters of the Yellow Sea, were reported 36,000 individuals in 2004-2005, and 14,000 individuals in 2011. The cause of rapid decline of finless porpoise is heavy impact of human activities (Turvey et al. 2007; Wang 2009). The primary impact is thought to be bycatch. Their main habitats are overlapping with the stow net fisheries which are the most dominant fisheries in that area. The stow net has accounted for more than 80 percent of finless porpoise bycatch in that area.

11 Contaminants

11.1 Persistent organic pollutants (POPs)

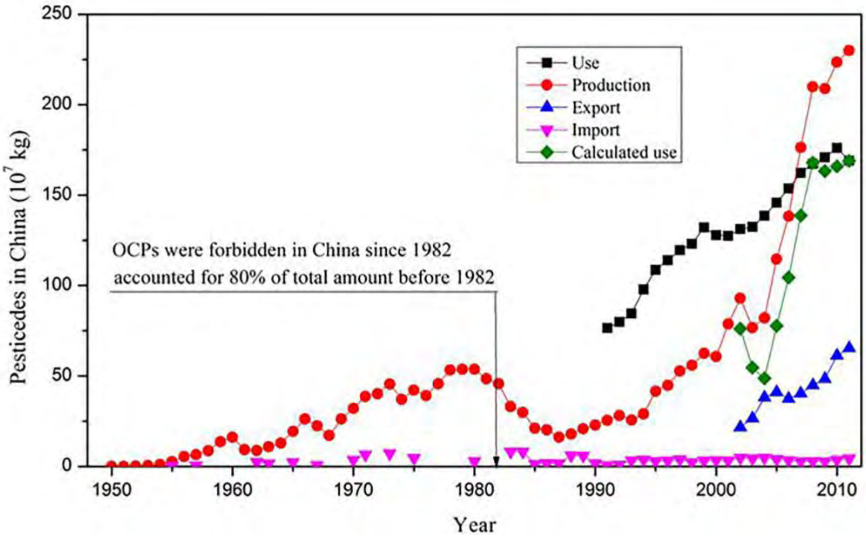

Figure R20-39. Historical production, use, export and import amounts of all pesticides in China (Grung, et al. 2015)

The historical production and use of pesticides in China are shown in Figure R20-39. Because organochlorine pesticides (OCPs) accounted for 80% of the total pesticides before 1982, the first regulation of OCPs in China in 1982 resulted in a sharp decrease in the production of total pesticides for five years. After that, the production of total pesticides (mostly non-OCPs) increased again. Previous researches (Xu et al. 2007; Hu et al. 2009; Zhao et al. 2010; Lin et al. 2012a, b; Zhou et al. 2014) investigated OCPs focusing on dichloro-diphenyl-trichloroethanes (DDTs) and hexachlorocyclohexanes (HCHs). Grung et al. (2015) assessed the risk levels of DDTs and lindane (HCHs in biota) using the Norwegian criteria and concluded that the concentrations in biota from some coastal areas could be classified as “bad” or “very bad” for DDT, including the Haihe Estuary and Yellow River Estuary. The risk in biota was much lower for HCH and the majority of the investigated areas could be classified as class I or II (background or good).

The existing data indicated that the polychlorinated biphenyls (PCBs). concentrations in the surface seawater in the Bohai Sea and East China Sea were lower than the EPA guidelines. Moreover, higher-level PCBs were detected in fish and shellfish samples collected from the Dalian Bay and Bohai Bay than in other coastal areas. However, in all the study areas, the residual levels of PCBs in marine organisms were far below the federal tolerance level of PCBs (2,000 ng/g wet wt.) provided by the USFDA (Xing et al. 2005).

China is one of the largest producer and consumer of polybrominated diphenyl ethers (PBDEs) in the world, and correspondingly the contamination of PBDEs in the marine environment has attracted a wide attention (Mai et al. 2005). The PBDEs concentrations in sediments of most coastal areas of China were relatively low compared with other countries (Table R20-2). The PBDEs residual levels in most coastal areas of China were also relatively lower than those of other countries. However, the concentrations of PBDEs from some polluted areas were comparable to/or even higher than those of developed regions (Table R20-2). The perfluorinated compounds (PFCs) concentrations in seawater of most coastal areas of China are also relatively low compared with other countries, perfluorooctanesulfonic acid (PFOS) and perfluorooctanoic acid (PFOA) are the dominant PFCs found in these seawaters (Figure R20-40). The contamination of PFCs in the Bohai Sea is more serious than other areas in China because of the presence of large chemical plants and rivers under high urban wastewater input (Chen et al. 2011). It was reported that the total concentration of nine PFAS (per- and polyfluoroalkyl substances) in the sediments in the different sampling areas were in the order of Bohai Sea > East China Sea > Yellow Sea (excluding the Bohai Sea) based on both the mean and median, with an increasing trend from the lower to the upper layers (Gao et al. 2014).

Table R20-2. Concentrations in different matrices collected from the coastal areas of China

Matrix	Research area	Result	Congener number	Reference
Seawater	Lingding Bay	∑PBDEs(mean): 5.0 ng/L	8	Luo et al., 2007
	Pearl River Delta	∑PBDEs(dissolved): 31.1-118.7 pg/L	17	Guan et al., 2007
	Hongkong	∑PBDEs(dissolved): 31.1-118.7 pg/L ∑PBDEs(particulate): 25.7-32.5 pg/L	8	Wurl et al., 2006
Sediment	Bohai Sea	∑PBDEs: 2.5 ng/g (dw)	14	Wang et al., 2009
	Yangtze River Delta	∑PBDEs: 13.6 ng/g (dw)	11	Chen et al., 2009
	Laizhou Bay	∑PBDEs: 240 ng/g (dw)	8	Jin et al., 2009
	Haihe Estuary	∑PBDEs: 60-2100 ng/g (dw)	27	Zhao et al., 2011
	Liaohe Estuary	∑PBDEs: 130-1980 ng/g (dw)	27	Zhao et al., 2011
Organism	Bohai Sea	∑PBDEs: 0.68 ng/g (dw)	14	Wang et al., 2009
	Laizhou Bay	∑PBDEs: 457.2 ng/g (dw)	8	Jin et al., 2009
	Liaodong Bay	∑PBDEs: 1.3-8.8 ng/g (dw)	15	Ma et al., 2013

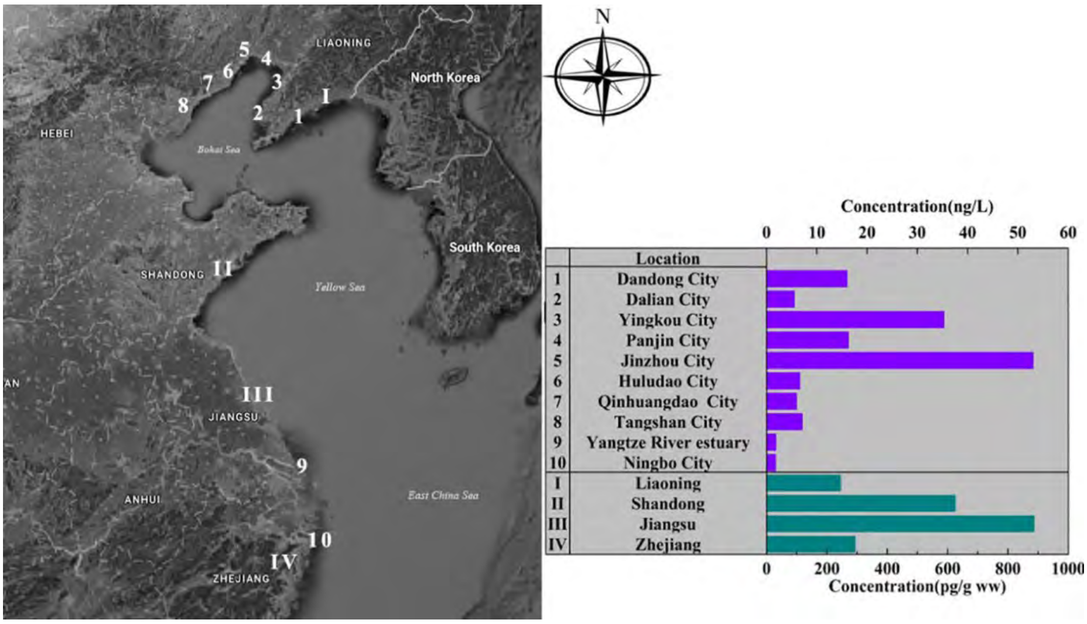

Figure R20-40. Concentration of perfluorinated compounds in the seawater of the coastal regions in China

In the Korean coastal waters in the Yellow Sea, POPs, including PCBs, DDTs, chlordane (CHL), HCHs, hexachlorobenzene (HCB) and PBDEs . were measured in the blubber of finless porpoises (n=52) collected in 2003 and in 2010 (Moon et al. 2010). For the blubber of finless porpoises (n=77) collected in 2010, the total concentrations of PCBs, DDTs, CHLs, HCHs, HCB and PBDEs were 50.5-3200 ng/g lw, 240-10100 ng/g lw, 11.3-300 ng/g lw, <LOQ-810 ng/g lw 1.6-100 ng/g lw and 48.0-1000 ng/g lw, respectively. The total concentrations of PCBs, OCPs and PBDEs in finless porpoises showed significant decreasing trends ($p<0.001$) between the sampling years of 2003 and 2010 (Figure R20-41). The reduction rates of these contaminants on average were 53%, 67%, 68%, 87%, 75%, and 62% for PCBs, DDTs, CHLs, HCHs, HCB and PBDEs, respectively. Of 52 finless porpoise samples collected in 2003, 27% exceeded the NOAEL (no observed adverse effect level) of immunosuppression by DDTs of harbor seals (De Swart et al., 1996) and 27% exceeded the total PCB-risk based toxic effect concentration (i.e. endocrine disruption and immunotoxicity) of 1300 ng/g lw (lipid weight) reported for harbor seals (Mos et al., 2010), implying adverse health effects on this species.

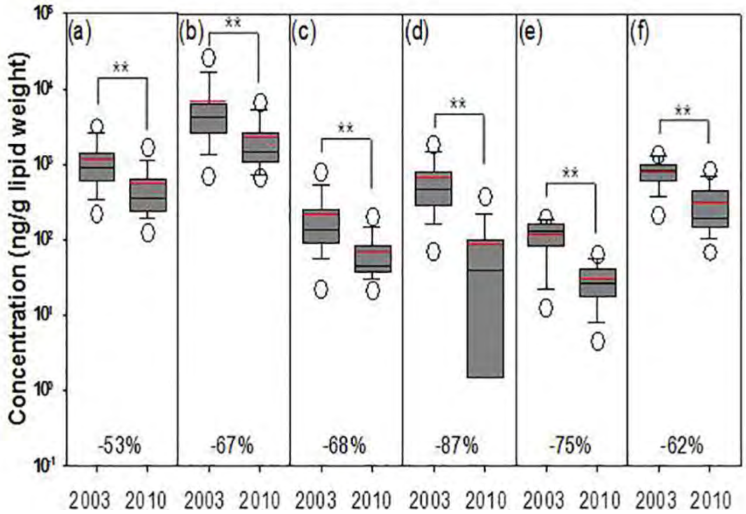

Figure R20-41. Temporal trends of (a) PCBs , (b) DDTs, (c) CHLs, (d) HCHs, (e) HCB, and (f) PBDEs of finless porpoises collected between 2003 and 2010 from Korean coastal waters. Significant percentage declines are indicated for each chemical groups (*p<0.05; **p<0.005). The box plot shows 10th, 25th, 50th, and 90th percentiles with error bars. The circles indicate the 5th percentile (lower) and the 95th percentile (upper). The arithmetic mean concentrations are given as red bars. The sample numbers for sex and growth groups were as follows: immature male (n=15), immature female (n=20), mature male (n=7), and mature female (n=10) collected in 2003 (total numbers=52); immature male (n=20), immature female (n=28), mature male (n=19), and mature female (n=10) collected in 2010 (total numbers=77).

From the same survey above, the total toxic equivalency (TEQ) levels of polychlorinated dibenzo-*p*-dioxins and dibenzofurans (PCDDs and PCDFs), non-ortho PCBs, and mono-ortho PCBs in the blubber of finless porpoises from both sampling years were lower than the o-observed-adverse-effect level (NOAEL) (62 pg TEQ/g) and lowest-observed-adverse-effect level (LOAEL) (209 pg TEQ/g) known to have immunomodulatory effects due to dioxin-like contaminants in harbor seals (*Phoca vitulina*; Ross et al. 1995). The total concentrations of PCDD/Fs and doxin-like PCBs in finless porpoises showed significant decreasing trends ($p<0.001$) between 2003 and 2010 (Figure R20-42). Based on the average concentrations of these contaminants, the reduction rates were 58%, 54%, 69%, and 60% for PCDDs, PCDFs, non-*ortho* and mono-*ortho* PCBs, respectively. In addition, the congener-specific temporal trends of PCDD/Fs and DL-PCBs also significantly decreased between the time-gap samples.

The spatial distribution of PCDD/Fs in bivalves showed relatively homogenous pattern compared to that of sediment contamination (Choi et al. 2010). A significant decreasing trend of PCDD/Fs was found in sediments from Korean coastal waters from 2010 to 2012 (Figure R20-43), suggesting the association with a strong regulation on PCDD/Fs in flue gas from waste incinerators in Korea (Ministry of Environment 2014). However, no significant temporal trends were found for PCDD/Fs in bivalves from Korean coastal waters. To evaluate ecotoxicological effects of PCDD/Fs in coastal sediment from Korea, sediment quality guidelines (SQGs) such as probable effect level (PEL: the concentration at which a large percentage of the benthic population shows a toxic response) and threshold effect level (TEL: the contamination concentration at which a toxic response has started to be observed in benthic organisms) from Florida State were used. Our evaluation showed that almost half of sediment samples (46%) had exceeding values of PCDD/Fs for the TEL (0.85 pg TEQ/g dry weight), implying ecotoxicological potential risks to marine organisms in Korean coastal waters.

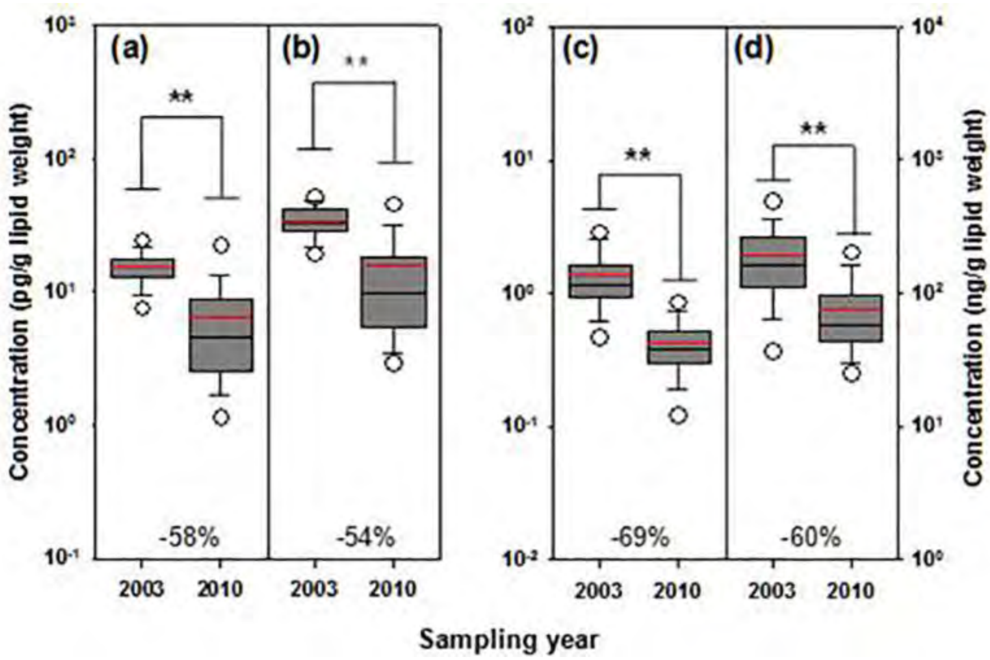

Figure R20-42. Temporal trends of (a) PCDDs , (b) PCDFs, (c) non-ortho PCBs, and (d) mono-ortho PCBs in finless porpoises collected between 2003 and 2010 from Korean coastal waters.

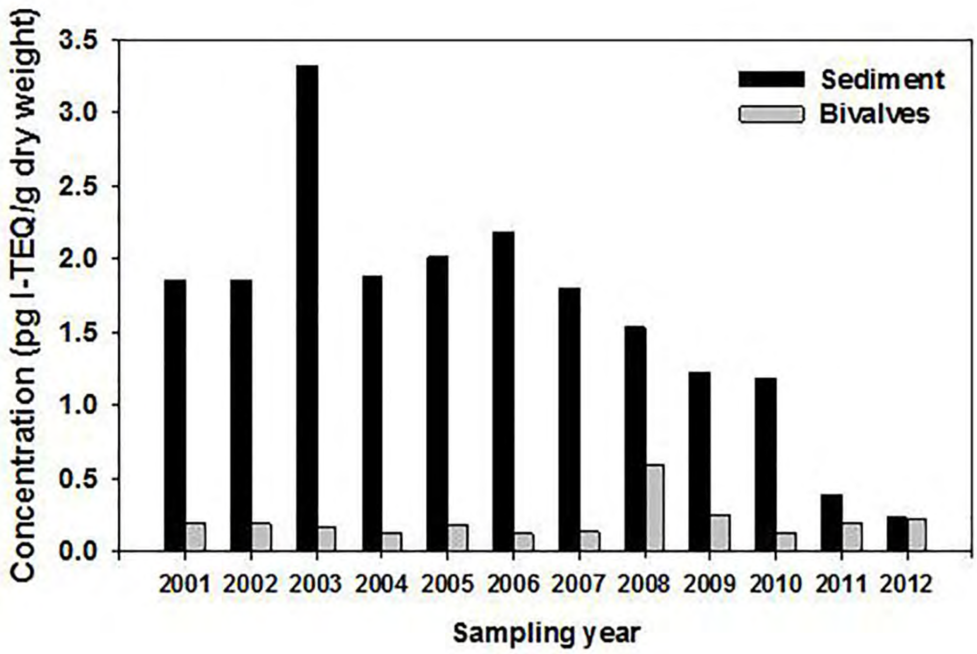

Figure R20-43. Temporal trends of mean concentrations of PCDD/Fs in sediment and bivalves (mussels and oysters) from 25 locations of Korean coastal waters over the period 2000-2012.

11.2 Polycyclic Aromatic Hydrocarbons (PAHs)

Overall, the PAHs levels in the seawater of the Chinese side of the Yellow Sea were comparable to or slightly lower than those of other coastal areas in the world (Alava et al. 2020). However, the values were highly variable from different surveys. For example, Zhang et al. (2016) reported that the surface water PAH levels in the Bohai Sea were higher than in many other locations in the world (Zhang et al. 2016). The levels of PAHs in the Yellow Sea were much lower (less than 20 ng l^{-1})(Jang et al. 2021). The concentrations of PAHs in sediments from the continental shelf off China were 27-224 ng/g (dw), with a median value of 57 ng/g. The sediments of the central Yellow Sea (53-224 ng/g, with a median of 129 ng/g) contained higher levels than those of the northern Yellow Sea (27-110 ng/g, with a median of 51 ng/g). Alava et al. (2020) argued that the PAHs in the North Chinese coastal sediment was relatively low compared with published data in other coastal regions worldwide. However, Wang et al. (2020) reported that the sediment PAH levels in the Bohai Sea were higher than those in the North Sea, the Yellow Sea, and the Baltic Sea. Those in the Yellow Sea were lower than in the Baltic Sea but higher than in the North Sea.

Surface sediments and two kinds of bivalve species including mussels (*Mytilus coruscus* and *M. edulis*) and oysters (*Crassostrea gigas*) were sampled at 25 locations around the Korean peninsula (western, southern, and eastern coasts of South Korea) over the period 2000-2012 (Figure R20-44). The total concentrations of PAHs in 2000-2012 ranged from 1.71 to 3,060 (mean: 216) ng/g dry weight for all of the sediment samples and from 4.36 to 2,653 (mean: 182) pg/g wet weight for all of the bivalve samples. The highest concentrations of PAHs in sediments and bivalves were observed in the southeastern part of Korea (Ulsan, Onsan, Busan, Masan, Jinhae Bays), which are the locations close to the largest industrial complexes and harbors. This result indicates that intensive industrial and shipping activities are the major contamination sources of PAHs in Korean coastal waters (Choi et al. 2010; 2011). No significant temporal trend was found for PAHs in sediments and bivalves from Korean coastal waters, implying the presence of wide ranging active sources of PAHs in coastal environment of Korea. The total concentrations of PAHs in sediments from Korean coastal waters did not exceed the effect range low (ERL) and effect range median (ERM) suggested by the National Oceanic and Atmospheric Administration (NOAA) as screening values for sediment quality (Long and Morgan 1990).

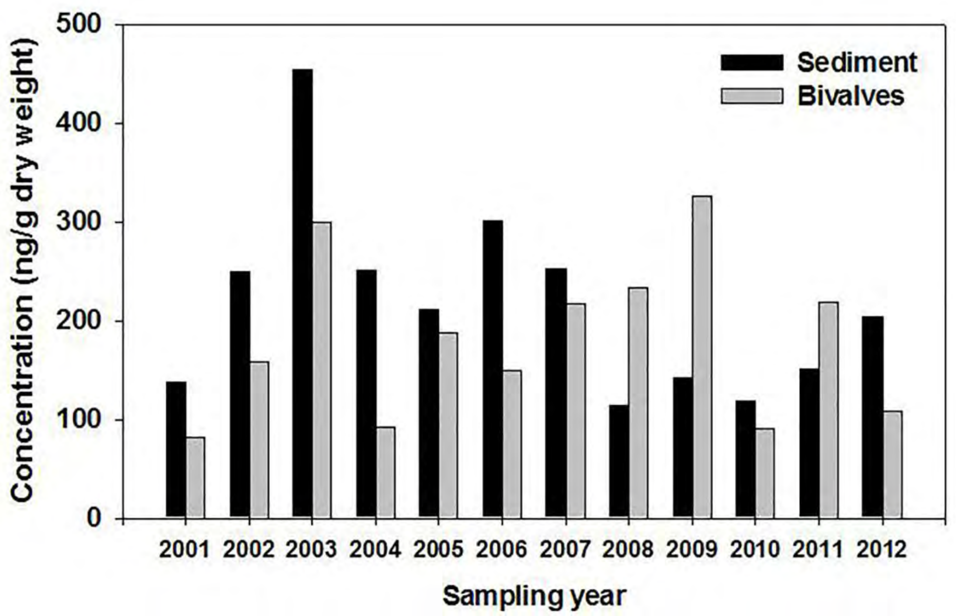

Figure R20-44. Temporal trends of mean concentrations of PAHs in sediment and bivalves (mussels and oysters) from 25 locations of Korean coastal waters during the period of 2000-2012.

11.3 Mercury

Marine bivalves such as mussels and oysters are often used as bioindicators for monitoring metal contamination in coastal environments. The Ministry of Oceans and Fisheries of Republic of Korea (MOF) has investigated the concentrations of trace metals in soft tissues of mussels (*Mytilus edulis*, n = 271) and oysters (*Crassostrea gigas*, n = 108) collected at 25 stations along the coast of Korea from 2000 to 2015. Relative to mussels, oysters have low Hg concentrations. Compared to the safety level (0.5 mg/kg-ww) of Hg for shellfish applied in Korea (MFDS 2015), the Hg concentrations in mussels and oysters were below the safety level in all samples except mussel of Onsan coast (in the eastern coast) in 2010. The mean Hg concentrations in mussel did not show any distinctive temporal trend during the monitoring periods (Figure R20-45), while the mean Hg concentrations in oyster were below 0.02 mg/kg-ww and were uniform over time since 2004 (Figure R20-46).

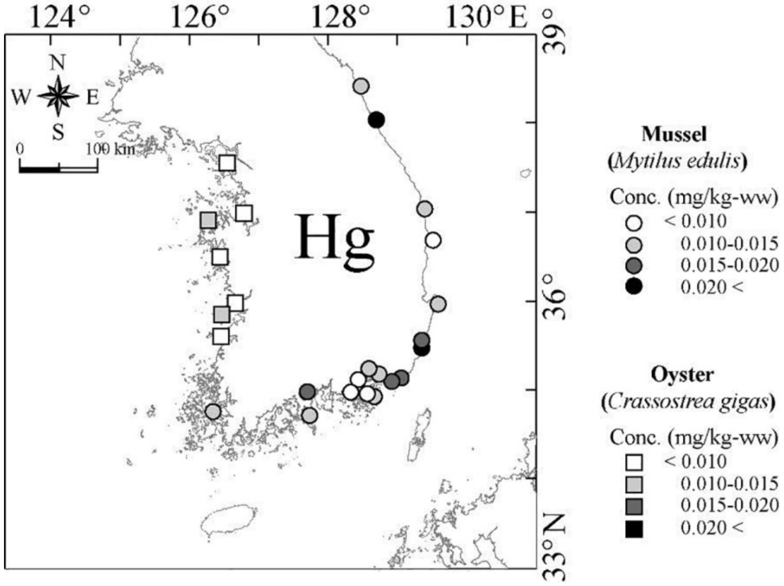

Figure R20-45. Horizontal distributions of mean Hg concentration in the tissues of mussels and oyster collected at 25 stations along the Korean coast from 2000 to 2015

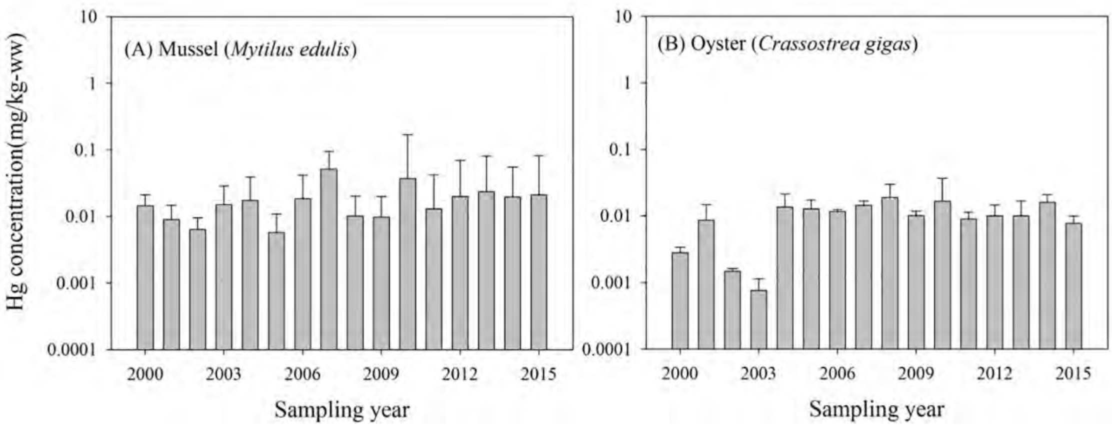

Figure R20-46. Annual variations of mean Hg concentration in the tissues of mussels and oysters collected

12 Climate Change, Ecosystem Considerations & Emerging Issues

The most salient climatic feature in the western North Pacific region has been the warming started in the middle of 1980s, which was also evident in the Yellow Sea. The warming has stopped in early 2000s. While the eastern North Pacific experienced the record-breaking marine heat wave in 2014-2015 period, there was no sign of any notable change in the sea temperature and salinity in the Yellow Sea during the focus period.

The Yellow Sea ecosystem, on the other hand, has been under progressing eutrophication, which can be characterized by continuous increases in the nutrient concentrations, chlorophyll-a, primary productivity and macroalgal blooms (green tides) until the early 2010s. At the same time, DO, pH, and the saturation state of aragonite have decreased. However, no significant changes have been observed in the macrobenthos communities, shorebird populations, and spotted seals (*Phoca larga)* and most contaminant (POPs, PAHs, Hg) levels are safe and stable except for a few hotspots in Chinese and Korean coasts.

Unexpectedly, HABs have been decreasing in both Chinese and Korean coastal waters. Also, the giant jellyfish blooms that peaked in 2003 did not occur in a significant density after 2007 in the eastern Yellow Sea. All the major factors proposed to explain these blooms, e.g., warming, eutrophication, fishing pressure, and man-made substrates, have not changed much and yet no large blooms were observed for the past 10 years. This conundrum suggests that our understanding of such processes is still very limited.

The green tides began to appear on a large scale since 2008 and still increase in distribution. It is still not clear what the long-term ecological impact of the annual recurrence of large-scale green tides is, although significant social and economic losses have been incurred due to the large accumulation of algal biomass on beaches and coastal waters.

Another emerging issue is the marine litter. Ever-increasing inputs of various forms of marine litter pose a significant threat to the marine ecosystem and human society. Nevertheless, surveys of marine litter are too limited to understand the basin-wide dynamics. Nor are assessed the impacts of marine litter on the marine ecosystem. Future studies of the dynamics, transportation, transformation and impacts on biota of the marine litter in the Yellow Sea basin are urgent.

The Yellow Sea ecosystem is arguably the one ecosystem among North Pacific ecosystems that is dominantly under the anthropogenic pressures. It serves as a good example of coastal marine ecosystems under increasing pressures from multiple drivers of human-induced environmental change.

References

Alava, J.J., Lukyanova, O.N., Ross, P.S., and Shim, W.J. (Eds.) 2020. Report of Working Group 31 on Emerging Topics in Marine Pollution. PICES Sci. Rep. No. 56, 161 pp.

Anonymous. 2004. Proceedings of “International Workshop on Jellyfish Bloom: China, Japan and Korea”, February 24. Yokohama, Japan.

Barter, M.A. 2002. Shorebirds of the Yellow Sea: Importance, threats, and conservation status. Wetlands International Global Series 9, International Wader Studies. Canberra, Australia.

Beardsley, R.C., Limeburner, R., Yu, H., and Cannon, G.A. 1985. Discharge of the Changjiang (Yangtze) River into the East China Sea. Cont. Shelf. Res. 4: 57-76.

Bolam, SG., Teresa, F. Fernandes., and Read, P. 2000. Effects of macroalgal mats on intertidal sandflats: An experimental study. J. Exp. Mar. Biol. Ecol. 249: 123-137.

Cabral, JA., Pardal, M., and Lopes, RJ. 1999. The impact of macroalgal blooms on the use of the intertidal area and feeding behaviour waders (Charadrii) in the Mondego estuary (west Portugal). Acta Oecologica. 20: 417-427.

Cetacean Research Institute, NIFS. 2018. Population survey of spotted seal in the Baengnyeong-do. Unpublished raw data.

Chen, C.-C., Gong, G.-C., and Shiah, F.-K. 2007. Hypoxia in the East China Sea: One of the largest coastal low-oxygen areas in the world. Mar. Environ. Res. 64: 399-408.

Chen ,CL., Lu, YL., Zhang, X., Geng, J., Wang, TY., and Shi, YJ. 2009. A review of spatial and temporal assessment of PFOS and PFOA contamination in China. Chem Ecol. 25:163–77.

Chen, Y., Shan, X., Jin, X., Johannessen, A., Yang, T., and Dai, F. 2017. Changes in fish diversity and community structure in the central and southern Yellow Sea from 2003 to 2015. Chin. J. Ocean. Limnol. 1-13. http://dx.doi.org/10.1007/s00343-018-6287-6.

Chen, Z.M., Gao, X.J., and Song, Z.G. 2011. Distribution of OCPs in surface intertidal sediments of Hangzhou Bay. China Environmental Science. 31: 321-327. (in Chinese)

Cho, B.C., Choi, J.-K., Chung, C.-S., and Hong, G.H. 1994. Uncoupling of bacteria and phytoplankton during a spring diatom bloom in the mouth of the Yellow Sea. Mar. Ecol. Prog. Ser. 115: 181-190.

Choi, H.-G., Moon, H.-B., Choi, M., and Yu, J. 2011. Monitoring of organic contaminants in sediments from the Korean coast: Spatial distribution and temporal trends (2001–2007). Mar. Pollut. Bull. 62: 1352-1361.

Choi, H.-G., Moon, H.-B., Choi, M., Yu, J., and Kim, S.-S. 2010. Mussel watch program for organic contaminants along the Korean coast, 2001-2007. Environ. Monit. Assess. 169: 473-485.

Choi, J.K., Park, Y.C., Kim, Y.C., Lee, Y.C., Son, S.K., Hwang, H.J., Han, B.S., and Jung, C.S. 1988. The study on the biological productivity of the fishing ground in the western coastal area of Korea, Yellow Sea. Bulletin of the National Fisheries Research Development Agency 42: 143-168.

CMAP (Climate Prediction Center Merged Analysis of Precipitation). 2019. http://www.cpc.ncep.noaa.gov/products/global_precip/html/wpage.cmap.html. last accessed date: March 4, 2019.

Costello, M.J., Coll, M., Danovaro, R., Halpin, P., Ojaveer, H., and Miloslavich, P. 2010. A census of marine biodiversity knowledge, resources, and future challenges. PLoS ONE 5: e12110. doi:10.1371/journal.pone.0012110

De Swart, R.L., Ross, P.S., Vos, J.G., and Osterhaus, A.D.M.E. 1996. Impaired immunity in harbor seals (*Phoca vitulina*) exposed to bioaccumulated environmental contaminants: review of a long-term feeding study Environ. Health Perspect. 104: 823-828.

Dong, J., and Shen, F. 1991. Estimates of historical population size of harbour seal (*Phoca largha*) in Liaodong Bay. Marine Sciences 3: 26-31.

Fu, M.Z., Wang, Z.L., Pu, X.M., Xu, Z.J., and Zhu, M.Y. 2012. Changes of nutrient concentrations and N:P:Si ratios and their possible impacts on the Huanghai Sea ecosystem. Acta Oceanologica Sinica. 31: 101–112.

Gao, Y., Fu, J., and Zeng, L. 2014. Occurrence and fate of perfluoroalkyl substances in marine sediments from the Chinese Bohai sea, Yellow sea, and East China sea. Environmental Pollution, 194: 60–68.

Garcia-Robledo, E., Corzo, A., and Papaspyrou, S. 2012. Photosynthetic activity and community shifts of microphytobenthos covered by green macroalgae. Environ Microbiol Rep. 4: 316-25.

Grung, M., Lin, Y., and Zhang, H. 2015. Pesticide levels and environmental risk in aquatic environments in China - A review. Environment International. 81: 87-97.

Guan,Y.F., Wang, J.Z., Ni, H.G., Luo, X.J., Mai, B.X., and Zeng, E.Y. 2007. Riverine inputs of polybrominated diphenyl ethers from the Pearl River Delta (China) to the coastal ocean. Environ. Sci. Technol. 41: 6007-6013.

Han, B.S., and Choi, J.K. 1991. A study on the environmental conditions and phytoplankton ecology in the tidal front area of the Yellow Sea. Yellow Sea Research. 4: 39-55.

Han, J.B. 2018. Population survey of spotted seal in the Liaodong Bay. Unpublished raw data.

Hare, SR. and Mantua, NJ. 2000. Empirical evidence for North Pacific regime shifts in 1977 and 1989. Prog. Oceanogr. 47: 103-145.

Hauxwell, J., Cebrian, J., and Furlong, C. 2001. Macroalgal canopies contribute to eelgrass (*Zostera marina*) decline in temperate estuarine ecosystems. Ecology. 82: 1007-1022.

He, X., Bai, Y., Pan, D., Chen, C.T.A., Cheng, Q., Wang, D., and Gong, F. 2013. Satellite views of the seasonal and interannual variability of phytoplankton blooms in the eastern China seas over the past 14 yr (1998–2011). Biogeosciences, 10: 4721–4739.

Hong, G.H., Chang, J., Kim, S.-H., Chung, C.S., Yang, S.R., Lee, J.H., and Kim, Y.I. 2003. East Asian marginal seas: river dominated ocean margin. Proceedings of the International Symposium on Oceanographic Environmental Change after Completion of the Changjiang Three-Gorges Dam. Jeju, Korea. May 15.

Hu, L., Zhang, G., and Zheng, B. 2009. Occurrence and distribution of organochlorine pesticides (OCPs) in surface sediments of the Bohai Sea, China. Chemosphere 77: 663-672.

Hwang, K. and Jung, S. 2012. Decadal changes in fish assemblages in waters near the Ieodo ocean research station (East China Sea) in relation to climate change from 1984 to 2010. Ocean Sci. J. 47: 83-94.

Ichikawa, H., and R. C. Beardsley. 2002. The current system in the Yellow and East China Seas, J. Oceanogr. 58: 77–92.

Jang, Y. L., Jeong, H., Kim, N.Y., Kim, G.B., 2021. Distribution of Freely Dissolved Polycyclic Aromatic Hydrocarbons in the Yellow Sea: Application of Improved Passive Sampling Technique. Ocean Science Journal, https://doi.org/10.1007/s12601-021-00039-7Jin, J., Liu, WZ., and Wang, Y. 2008 Levels and distribution of polybrominated diphenyl ethers in plant, shellfish and sediment samples from Laizhou Bay in China. Chemosphere 71:1043–1050.

Jin, J., Wang, Y., Yang, C., Hu, J., Liu, W., and Cui, J. 2009. Polybrominated diphenyl ethers in the serum and breast milk of the resident population from production area, China. Environ. Int. 35: 1048-52.

Jones, M., and Pinn, E. 2006. The impact of a macroalgal mat on benthic biodiversity in Poole Harbour. Mar. Pollut. Bull. 53: 63-71.

Jung, S. 2014. Asynchronous responses of fish assemblages to climate-driven ocean regime shifts between the upper and deep layer in the Ulleung Basin of the East Sea from 1986 to 2010. Ocean Sci. J. 49: 1-10.

Jung, S., Pang, I., Lee, J., Choi, I., and Cha, H.K. 2014. Latitudinal shifts in the distribution of exploited fishes in Korean waters during the last 30 years; a consequence of climate change. Rev. Fish Biol. Fish. 24: 443-462.

Jung, S., Pang, I., Lee, J., and Lee, K. 2016. Climate-change driven range shifts of anchovy biomass projected by bio-physical coupling individual based model in the marginal seas of East Asia. Ocean Sci. J. 51: 563-580.

Kang, J.-h., Kang, T.-h., Cho, H.-j., Lee, S.-w, Kim, I-g., Yoo, S., and Seung-hwa. 2008. Study on the Breeding Status of the Natural Monument Islet (Chilbaldo, Sasudo, Nando, Hongdo), Kor. J. Orni. 15:169-175.

Kang, Y.S., Choi, J.-K., Chung, K. H., and Park, Y.-C. 1992. Primary productivity and assimilation number in the Kyonggi Bay and the mid-eastern coast of Yellow Sea. Journal Oceanology of Korea 27: 237-246.

Kang, Y.S. 2008. Seasonal variation in zooplankton related to North Pacific Regime Shift in Korea Sea. J. Kor. Fish. Soc. 41: 493-504.

Kang, Y.S., and Lee, S.S. 1991. Seasonal fluctuations of zooplankton biomass in the adjacent sea of Korea. Bulletin of the National Fisheries Research and Development Agency 45: 13-21.

Kang, Y.S., and Ohman, M.D. 2014. Comparison of long-term trends of zooplankton from two marine ecosystems across the North Pacific: Northeastern Asian marginal sea and Southern California current system. California Cooperative Oceanic Fisheries Investigations Reports. 55:169-182.

Katoh, O., Nakagawa, N., Matsui, S., Yamada, H., and Watanabe, T. 2006. Long-term fluctuations of water temperature in the Japan Sea and the Tsushima strait shown by data from prefectural observations along the coastal and offshore measurement lines. Bulletin on Coastal Oceanography 44: 19-24.

KCJRG (Korea-China Joint Research Group). 2004. Report of the Yellow Sea environment cooperative research between Korea and China, 2003.

Kim, S., and Khang, S.H. 2000. The Yellow Sea, In Sheppard, C. (ed.), Seas at the Millennium: An Environmental Evaluation, Elsevier Science. 487-498.

Kim, Y. S., Chan, J.J., and Yeh, S.-W. 2018. Recent Surface Cooling in the Yellow and East China Seas and the Associated North Pacific Climate Regime Shift. Cont. Shelf. Res. 15: 43–54. https://doi.org/10.1016/j.csr.2018.01.009.

Koh, E.H., Joo, H.W., Lee, D.W., Cha, H.K., and Choi, J.H. 2016. Community composition and distribution of fish species collected by bottom trawl from the middle of the Yellow Sea in summer (2008–2014). Kor. J. Fish. Aquat. Sci. 49: 849-855.

Koh, C.H., and Khim, J.S. 2014. The Korean tidal flat of the Yellow Sea: physical setting, ecosystem and management. Ocean Coast. Manage. 102: 398-414.

Korea National Park Research Institute. 2014. 2013~2014 Bird survey and research of Korea National Park (written in Korean)

Korea National Park Research Institute. 2015. 2015~2016 Bird survey and research of Korea National Park (written in Korean)

Korea National Park Research Institute. 2018. 2018 Monitoring impacts of climate changes on ecosystem (publishing, written in Korean)

Le Luherne, E., Réveillac, E., and Ponsero, A., 2016. Fish community responses to green tides in shallow estuarine and coastal areas. Estuar. Coast. Shelf. Sci. 175: 79-92.

Lee, C. 2004. Review of the fish-fauna of the West Sea of Korea. Korean Journal of Ichthyology 16: 60-74.

Lee, D.P., Lee K.G., and Nam D.H. 2012. Population declines and heavy metal exposure of Swinhoe's storm Petrels (*Oceanodroma monorhis*) breeding on the Southwest coast of Korea, Mar. Pollut. Bull. 64: 2645-2649.

Li, H.M., Zhang, C.S., Han, X.R., and Shi, X.Y. 2015. Changes in concentrations of oxygen, dissolved nitrogen, phosphate, and silicate in the southern Yellow Sea, 1980-2012: Sources and seaward gradients. Estuar. Coast. Shelf Sci. 163: 44–55. https://doi.org/10.1016/j.ecss.2014.12.013

Lie, H.-J., and Cho, C.-H. 2002. Recent advances in understanding the circulation and hydrography of the East China Sea. Fish. Oceanogr. 11: 318-328.

Lin, T., Hu. L., and Shi, X. 2012a. Distribution and sources of organochlorine pesticides in sediments of the coastal East China Sea Mar. Pollut. Bull. 64: 1549-1555.

Lin, T., Li, J., and Xu, Y. 2012b. Organochlorine pesticides in seawater and the surrounding atmosphere of the marginal seas of China: Spatial distribution, sources and air-water exchange. Sci. Total Environ. 435-436: 244-252.

Liu, R. 2011. Progress of marine biodiversity studies in China seas. Biodiversity Science. 19: 614–626.

Liu, J.Y. 2013. Status of Marine Biodiversity of the China Seas. PLoS ONE 8: e50719. doi:10.1371/journal.pone.0050719

Liu, D., Keesing, JK., and He, P. 2013. The world's largest macroalgal bloom in the Yellow Sea, China: Formation and implications. Estuar. Coast. Shelf. Sci. 129: 2-10.

Long, E.R., and Morgan, L.G. 1990. The potential for biological effects of sediment-sorbed contaminants tested in the National Status and Trends Program. NOAA Technical Memorandum NOS OMA 52. National Oceanic and Atmospheric Administration. Seattle, Washington, United States.

Luo, Q., Cai, Z.W., and Wong, M.H. 2007. Polybrominated diphenyl ethers in fish and sediment from river polluted by electronic waste. Sci. Total Environ. 383: 115-127.

Ma, X., Zhang, H., Yao, Z., Zhao, X., Wang, L., Wang, Z., Chen, J., and Chen, J. 2013. Bioaccumulation and trophic transfer of polybrominated diphenyl ethers (PBDEs) in a marine food web from Liaodong Bay, North China. Mar. Pollut. Bull. 74: 110e115.

Mai, B.X., Chen, S.J., and Luo, X.J. 2005. Distribution of polybrominated diphenyl ethers in sediments of the Pearl River Delta and Adjacent South China Sea. . Environ. Sci. Technol. 39: 3521-3527.

MFDS (Ministry of Food and Drug Safety). 2015. Korean Food Code – Chapter 6 A standards for marine products. p.1505 (in Korean?)

Ministry of Environment. 2014. Report on the effect of the regulation to dioxin emission, Ministry of Environment of Korea, Seoul, Korea (in Korean).

Moon, H.-B., Choi, H.-G., An, Y.-R., Park, G.-J., Choi, Moon, D.-Y., and Kannan, K. 2010. Contamination status and accumulation features of PCDDs, PCDFs and dioxin-like PCBs in finless porpoises (*Neophocaena phocaenoides*) from Korean coastal waters. Journal of Hazardous Materials 183: 799-805.

Mos, L., Cameron, M., Jeffries, S.J., Koop, B.F., and Ross, P.S. 2010. Risk-based analysis of polychlorinated biphenyl toxicity in harbor seals. Integr. Environ. Assess. Manag. 6: 631-640.

Nam, K., and Yoo, J. 2017. Population trend of a colonial breeding seabird, under high predation risk. Proceedings of the Korean Ornithological Society meeting in autumn.

Nam, K., Lee, K., Hwang, J., and Yoo, J. 2014. Variation in Breeding Burrows of Streaked Shearwaters Breeding in Sasu Island, and Predation Rates by Norway Rats, Ocean and polar research 36: 49-57 (written in Korean with English abstract).

NIBR. 2008. Wintering waterbird census of Korea. National Institute of Biological Resources (in Korean).

NIBR. 2009. Wintering waterbird census of Korea. National Institute of Biological Resources (in Korean).

NIBR. 2010a. A study on the migration route and the status of wintering and stop over ecology of migratory birds National Institute of Biological Resources. National Institute of Biological Resources (in Korean).

NIBR. 2010b. Wintering waterbird census of Korea. National Institute of Biological Resources (in Korean).

NIBR. 2011a. A study on the migratory route and the status of wintering and stop over sites of migratory birds. National Institute of Biological Resources (in Korean).

NIBR. 2011b. Wintering waterbird census of Korea. National Institute of Biological Resources (in Korean).

NIBR. 2012a. A study on the migratory route and the status of wintering and stop over sites of migratory birds. National Institute of Biological Resources (in Korean).

NIBR. 2012b. Wintering waterbird census of Korea. National Institute of Biological Resources (in Korean).

NIBR. 2013a. A study on the migratory route and the status of wintering and stop over sites of migratory birds. National Institute of Biological Resources (in Korean).

NIBR. 2013b. Wintering waterbird census of Korea. National Institute of Biological Resources (in Korean).

NIBR. 2014a. Migratory route study for HPAI Surveillance and monitoring of migratory birds in Korea. National Institute of Biological Resources (in Korean).

NIBR. 2014b. Wintering waterbird census of Korea. National Institute of Biological Resources (in Korean).

NIBR. 2015a. Monitoring of passage migratory birds in Korea. National Institute of Biological Resources (in Korean).

NIBR. 2015b. Wintering waterbird census of Korea. National Institute of Biological Resources (in Korean).

NIBR. 2016. Wintering waterbird census of Korea. National Institute of Biological Resources (in Korean).

Park, C. 2013. A study on the breeding ecology of murrelets at Gugul-do Islet, Natural monument. National Institute of Biological Resources (in Korean).

Park, J. 2000. Vertical distribution and primary productivity of phytoplankton in the Yellow Sea in spring time, M.S. thesis, Inha University, Korea.(in Korean?)

Park, J., Song, S.J., Ryu, J., Kwon, B-O., Hong, S., Bae, H., Choi, J-W., and Khim, J.S. 2014. Macrozoobenthos of Korean tidal flats: A review on species assemblages and distribution. Ocean. Coast. Manag. 102: 483-492.

Park, K.J., Sohn, H., An, Y.R., Kim, H.W., and An, D.H. 2015. A New Abundance Estimate for the Finless Porpoise *Neophocaena asiaeorientalis* on the West Coast of Korea: An Indication of Population Decline. Fish. Aquatic. Sci. 18: 411-416.

Qi, L., Hu, C.M., and Xing, Q.G.l. 2016. Long-term trend of *Ulva prolifera* blooms in the western Yellow Sea. Harmful Algae. 58: 35-44.

Rabouille, C., Conley, D.J., Dai, M.H., Cai, W.J., Chen, C.T.A., Lansard, B., Green, R., Yin, K., Harrison, P.J., Dagg, M., and McKee, B. 2008. Comparison of hypoxia among four river-dominated ocean margins: The Changjiang (Yangtze), Mississippi, Pearl, and Rhône rivers. Cont. Shelf. Res. 2812: 1527-1537.

Rebstock, G., and Kang, Y.S. 2003. A comparison of three marine ecosystems surrounding the Korean peninsula: Responses to climate change. Prog. Oceanogr. 59: 357-379.

Rogers, J.C. 1981. The North Pacific Oscillation. Journal of Climate 1: 39-57.

Ross, P.S., De Swart, R.L., Reijnders, P.J.H., Van Loveren, H., Vos, J.G., and Osterhaus, A.D.M.E. 1995. Contaminant-related suppression of delayed-type hypersensitivity and antibody responses in harbor seals fed herring from the Baltic sea. Environ. Health Perspect. 103: 162-167.

Schramm, W. 1999, Factors influencing seaweed responses to eutrophication some results from EU-project EUMAC. Journal of Applied Phycology. 11: 69–78.

Sea Around Us. 2017. Sea Around US. http://www.seaaroundus.org. Accessed November 6, 2017

Shan, X., Li, X., Yang, T., Sharifuzzaman, SM., Zhang, G., Jin, X., and Dai, F. 2017. Biological responses of small yellow croaker (*Larimichthys polyactis)* to multiple stressors: a case study in the Yellow Sea, China. Acta. Oceanol. Sin. 36: 39-47.

State Oceanic Administration, People's Republic of China. 2019. http://dx.doi.org/10.1007/s13131-017-1091-2. last accessed date: August 30, 2018.

Song, T.Y. 1999. Monthly variation of phytoplankton community structure and pigment in the Kyeonggi Bay, Korea. M.S. thesis, Inha University. (In Korean?)

Sun, S., Li, Y., and Sun, X. 2012. Changes in the small-jellyfish community in recent decades in Jiaozhou Bay, China Chin. J. Ocean. Limnol. 30: 507-518.

Sun, S., Wang, F., and Li, C.. 2008. Emerging Challenges: Massive Green Algae Blooms in the Yellow Sea. Nature Precedings: 1-5.

Tang, D., Di, B., Wei, G., Ni, H., Oh, I.S., Wang, S. 2006. Spatial, seasonal and species variations of harmful algal blooms in the South Yellow Sea and East China Sea. Hydrobiologia 568: 245-253.

Tang, Q. 1989. Changes in the biomass of the Yellow Sea ecosystem. pp. 7-35 Sherman, K. and Alexander, L.M. (eds.), In Biomass Yields and Geography of Large Marine Ecosystems, AAAS Selected Symposium 111, Westview Press, Boulder, CO, USA

The Yellow Sea Ecoregion Initiative. 2001. Yellow Sea Ecoregion: Reconnaissance Report on Identification of Important Wetland and Marine Areas for Biodiversity Conservation. Volume 2: South Korea. The Yellow Sea Ecoregion Initiative: a joint project of WWF-Japan, Wetlands & Birds Korea and Wetlands International-China Programme.

Tian, Y., Kidokoro, H., Watanabe, T., and Iguchi, N. 2008. The late 1980s regime shift in the ecosystem of Tsushima warm current in the Japan/East Sea: evidence from historical data and possible mechanisms. Prog. Oceanogr. 77: 127-145.

Turvey, S.T., Pitman, R.L., Taylor, B.L., Barlow, J., Akamatsu, T., Barrett, L.A. and Wei, Z. 2007. First human-caused extinction of a cetacean species?. Biol. Lett. 3: 537-540.

UNDP/GEF (United Nations Development Programme/Global Environment Facility). 2007. The Yellow Sea: Analysis of Environmental Status and Trends, Volume 3: Regional Synthesis Reports. UNDP/GEF Yellow Sea Project, Ansan, Republic of Korea. UNDP/GEF (United Nations Development Programme/Global Environment Facility).

Valiela, .I, McClelland, J., Hauxwell, J., Behr, PJ., Hersh, D., and Foreman, K. 1997. Macroalgal blooms in shallow estuaries: controls and ecophysiological and ecosystem consequences. Limnol. Oceanogr. 42:1105–1118.

Wang, D. 2009. Population status, threats and conservation of the Yangtze finless porpoise. Chinese Sci. Bull. 54: 3473-3484.

Wang, P., Mi, W., Xie, Z., Tang, J., Apel, C., Joerss, H., Ebinghaus, R., and Zhang, Q. 2020. Overall comparison and source identification of PAHs in the sediments of European Baltic and North Seas, Chinese Bohai and Yellow Seas. Science of the Total Environment, https://doi.org/10.1016/ j.scitotenv.2020.139535

Wang, P., Zhang, Q.H., Wang, Y.W., Wang, T., Li, X.M., Li, Y.M., Ding, L., and Jiang, G.B. 2009. Altitude dependence of polychlorinated biphenyls (PCBs) and polybrominated diphenyl ethers (PBDEs) in surface soil from Tibetan Plateau, China. Chemosphere 76: 1498–1504.

Wang, XH., Li, L., and Bao, X. 2009b. Economic cost of an algae bloom cleanup in China's 2008 Olympic sailing venue. Eos 90: 238-239.

Wang, Z., Xiao, J., and Fan, S. 2015. Who made the world's largest green tide in China?-an integrated study on the initiation and early development of the green tide in Yellow Sea. Limnol. Oceanogr. 60: 1105-1117.

Wei, Q.S., Yao, Q.Z., Wang, B.D., Wang, H.W., and Yu, Z.G. 2015. Long-term variation of nutrients in the southern Yellow Sea. Cont. Shelf. Res. 111: 184-196.

Won, C., and Yoo, B. H. 2004. Abundance, seasonal haul-out patterns and conservation of spotted seals *Phoca largha* along the coast of Bak-ryoung Island, South Korea. Oryx 38: 109-112.

Working Group on Governance of the PR China (2019). Interim Review Report on the Progress of Implementation of the National Strategic Action Programme for YSLME 2009-2020 of the People's Republic of China. YSLME Phase II Project, 112pp.

Wurl, O., Lam, P.K.S., and Obbard, J.P., 2006. Occurrence and distribution of polybrominated diphenyl ethers (PBDEs) in the dissolved and suspended phases of the sea-surface microlayer and seawater in Hong Kong, China. Chemosphere 65: 1660–1666.

Xing, Y., Lu, Y., Dawson, R. W., Shi, Y., Zhang, H., Wang, T., Liu, W., and Ren, H. 2005. A spatial temporal assessment of pollution from PCBs in China. Chemosphere 60: 731-739.

Xing, Q., Tosi, L., and Braga, F. 2015. Interpreting the progressive eutrophication behind the world's largest macroalgal blooms with water quality and ocean color data. Nat. Hazards. 78: 7-21.

Xu, X., Yang, H., and Li, Q. 2007. Residues of organochlorine pesticides in near shore waters of LaiZhou Bay and JiaoZhou Bay, Shandong Peninsula, China. Chemosphere 68: 126-139.

YSLME (Yellow Sea Large Marine Ecosystem), 2010. Regional Cruise Report. Draft1_2nd. 100pp.

Ye, N-H., Zhang, X-W., and Mao, Y-Zl. 2011. 'Green tides' are overwhelming the coastline of our blue planet: taking the world's largest example. Ecol. Res. 26: 477-485.

Yeh, S.-W. and Kim, C.-H. 2010. Recent warming in the Yellow and East China Sea during the boreal winter. Cont. Shelf. Res. 30: 1428-1434.

Yoo, S. and Shin, K. 1995. The primary productivity off the coast of Taeahn. Ocean Research 17: 91-99.

Yoo, S., Kong, C.E., Son, Y.B., and Ishizaka, J. 2019. A critical re-assessment of the primary productivity of the Yellow Sea, East China Sea and Sea of Japan/East Sea Large Marine Ecosystems. Deep Sea Res. Part II, 163:6-15,https://doi.org/10.1016/j.dsr2.2018.05.021

Zhang, A., Zhao, S., Wang, L., Yang, X., Zhao, Q., Fan, J., and Yuan, X., 2016. Polycyclic aromatic hydrocarbons (PAHs) in seawater and sediments from the northern Liaodong Bay, China. Marine Pollution Bulletin, http://dx.doi.org/10.1016/j.marpolbul.2016.09.005

Zhang, C., Lee, J., Kim, S., and Oh, J. 2000. Climatic regime shifts and their impacts on marine ecosystem and fisheries resources in Korean waters. Prog. Oceanogr. 47: 171-190.

Zhang, CI., Lee, JB., Seo, YI., Yoon, SC., and Kim, S. 2004. Variations in the abundance of fisheries resources and ecosystem structure in the Japan/East Sea. Prog. Oceanogr. 61: 245-265.

Zhai, W.-D., Zheng, N., Huo, C., Xu, Y., Zhao, H.-D., Li, Y.-W., Zang, K.-P., Wang, J.-Y., and Xu, X.-M. 2014. Subsurface pH and carbonate saturation state of aragonite on the Chinese side of the North Yellow Sea: seasonal variations and controls, Biogeo sciences. 11: 1103–1123.

Zhao, L., Hou, H., and Zhou, Y. 2010. Distribution and ecological risk of polychlorinated biphenyls and organochlorine pesticides in surficial sediments from Haihe River and Haihe Estuary Area, China. Chemosphere 78: 1285-1293.

Zhao, X., Hamre, J., Li, F., Jin, X., and Tang, Q. 2003. Recruitment, sustainable yield and possible ecological consequences of the sharp decline of the anchovy (*Engraulis japonicus*) stock in the Yellow Sea in the 1990s. Fish. Oceanogr. 12: 495-501.

Zhao, XF., Zhang, HJ., Ni, YW., Lu, XB., Zhang, XP., and Su, F. 2011. Polybrominated diphenyl ethers in sediments of the Daliao River Estuary, China: levels, distribution and their influencing factors. Chemosphere 82:1262–7.

Zhou, M., Liu, D., and Anderson, DM. 2015. Introduction to the Special Issue on green tides in the Yellow Sea. Estuar. Coast. Shelf. Sci. 163: 3-8.

Zhou, M.-J., Shen, Z.-L., and Yu, R.-C. 2008. Responses of a coastal phytoplankton community to increased nutrient input from the Changjiang (Yangtze) River. Cont. Shelf. Res. 28: 1483-1489.

Zhou, S., Yang, H., and Zhang, A. 2014. Distribution of organochlorine pesticides in sediments from Yangtze River Estuary and the adjacent East China Sea: Implication of transport, sources and trends. Chemosphere 114: 26-34